Search for Stochastic Gravitational Wave Background

Kin-Wang Ng (吴建宏)

Institute of Physics &
Institute of Astronomy and Astrophysics
Academia Sinica

Cosmology Frontier in Particle Physics: Astroparticle Physics and Early Universe / International Joint Workshop on the SM and Beyond
NTU/NTHU, Oct 12-15, 2021

+ Guo-Chin Liu (Tamkang University)+Wolung Lee (NTNU)
+ Yu-Kuang Chu (AS and UW Milwaukee) + Shu-Lin Cheng (AS)

Outline

- Stochastic gravitational-wave background (GWB)
- Astrophysical and cosmological sources
- Observation
- Our works – overlap reduction functions (ORFs) for polarized GWB
- Perspectives

Cosmological GW spectral energy density

tion h_{ij} is gauged to be transverse-traceless. The latter can be decomposed into two polarization unit tensors as

$$h_{ij}(\eta,\vec{x}) = \sum_{\lambda=+,\times} \int \frac{d^3\vec{k}}{(2\pi)^{\frac{3}{2}}} h_\lambda(\eta,\vec{k}) \epsilon_{ij}^{\lambda}(\hat{k}) e^{i\vec{k}\cdot\vec{x}}, \qquad (2)$$

where $h_\lambda(\eta,\vec{k})$ is a Gaussian random field that defines the power spectrum of tensor perturbation,

$$\langle h_\lambda(\eta,\vec{k}) h^*_{\lambda'}(\eta,\vec{k}')\rangle = \delta(\vec{k}-\vec{k}') \frac{2\pi^2}{k^3} \mathcal{P}_h^{\lambda\lambda'}(\eta,k). \qquad (3)$$

In the following, we will assume that $\mathcal{P}_h^{\lambda\lambda'}(\eta,k) = \delta_{\lambda\lambda'}\mathcal{P}_h(\eta,k)$. Then, the spectral energy density of the GWs relative to the critical density is given by

$$\Omega_{\rm GW}(\eta,k,\hat{k}) \equiv \frac{k}{\rho_c}\frac{d\rho_{\rm GW}}{dk d^2\hat{k}} = \frac{1}{96\pi}\left(\frac{k}{aH}\right)^2 \bar{\mathcal{P}}_h(\eta,k), \quad (4)$$

where $\rho_c = 3M_p^2H^2$ and the overbar denotes taking a time-average. For k-modes that re-enter the horizon

Cosmological sources for gravitational waves

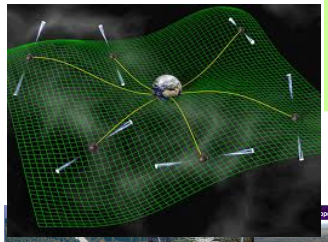

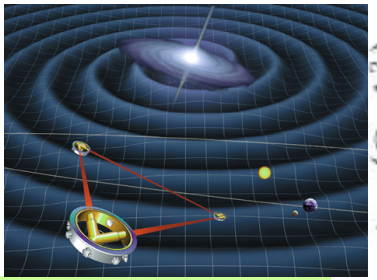

Astrophysical sources

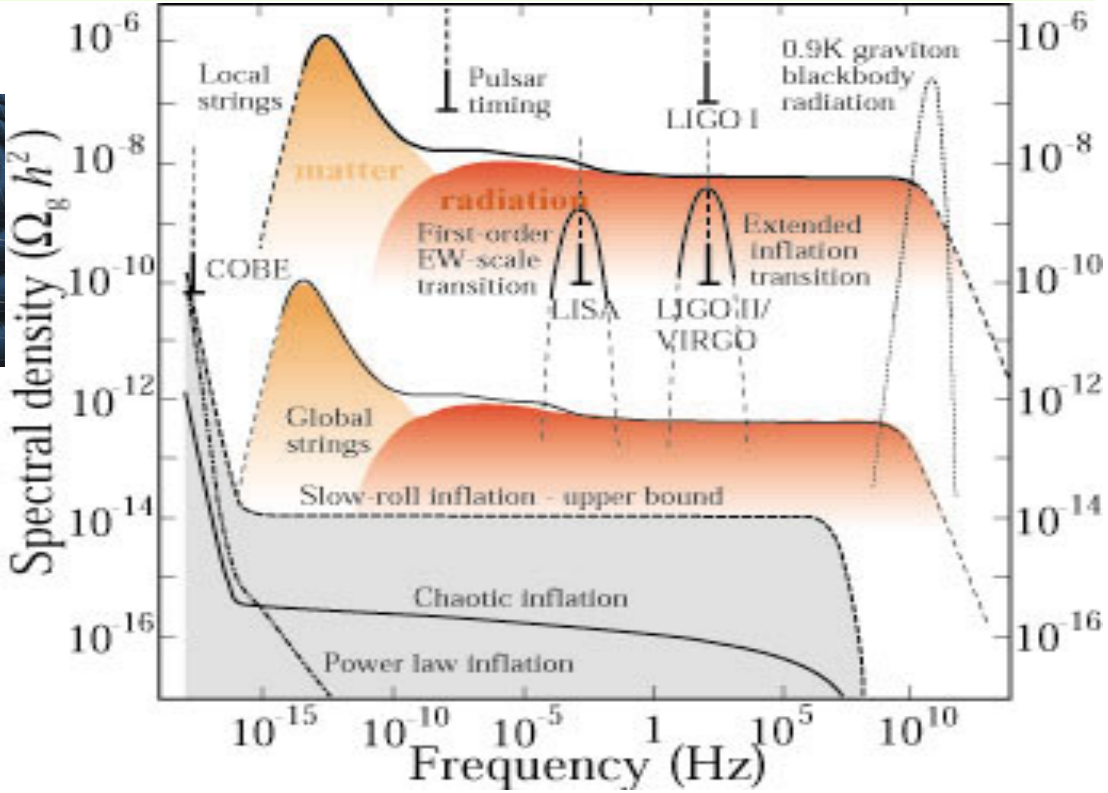

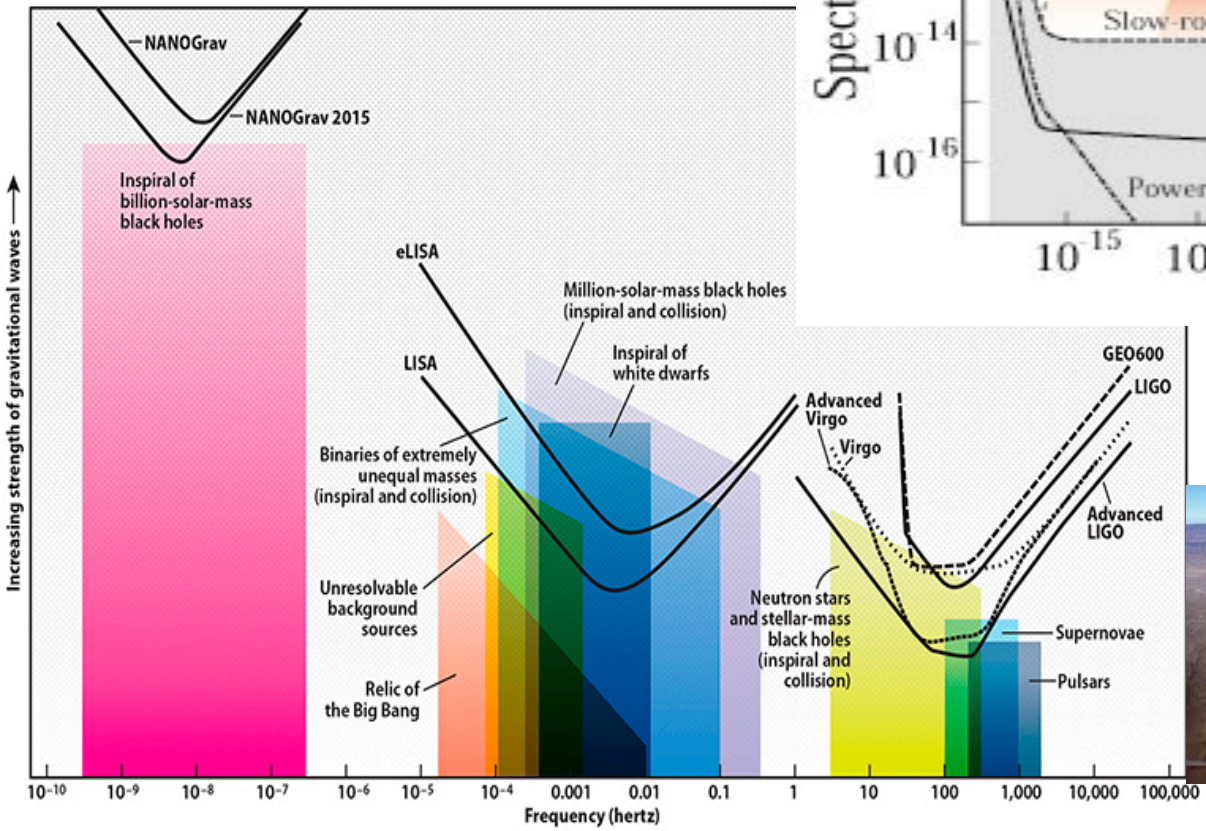

Current Upper Bounds

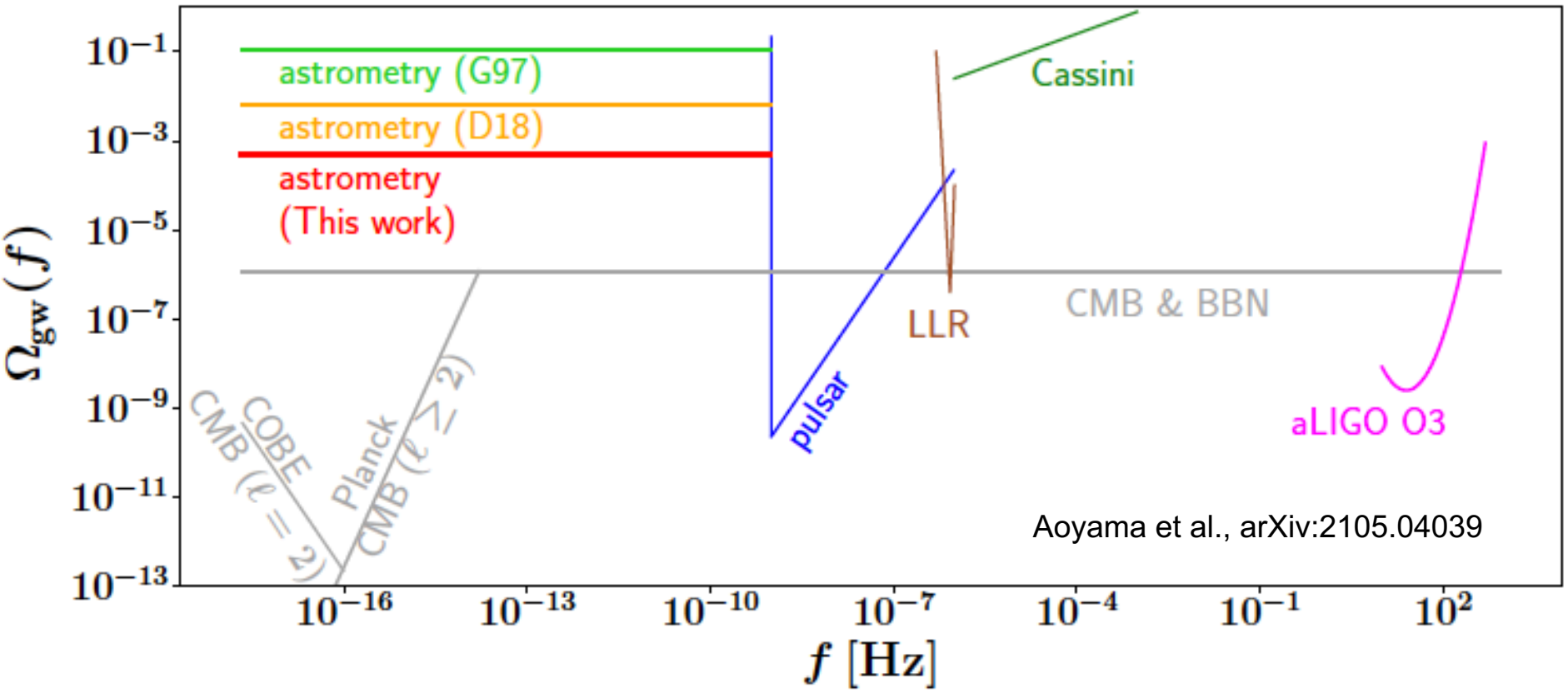

Aoyama et al., arXiv:2105.04039

CMB – anisotropy + B-mode polarization
CMB&BBN – extra degrees of freedom
Cassini+LLR – radar launching

aLIGO – direct detection of wave strain
Pulsar – Shapiro time delay
Astrometry – gravitational lensing effect

North American Nanohertz Observatory for Gravitational Waves

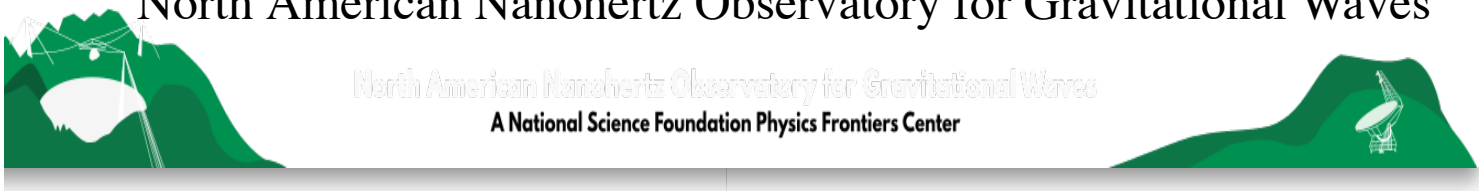

The NANOGrav 12.5-year Data Set: Search For An Isotropic Stochastic Gravitational-Wave Background

arXiv:2009.04496 9 Sep 2020

We search for an isotropic stochastic gravitational-wave background (GWB) in the 12.5-year pulsar timing data set collected by the North American Nanohertz Observatory for Gravitational Waves (NANOGrav). Our analysis finds strong evidence of a stochastic process, modeled as a power-law, with common amplitude and spectral slope across pulsars. The Bayesian posterior of the amplitude for a $f^{-2/3}$ power-law spectrum, expressed as characteristic GW strain, has median 1.92×10^{-15} and 5%–95% quantiles of 1.37–2.67×10^{-15} at a reference frequency of $f_{\rm yr} = 1\ {\rm yr}^{-1}$. The Bayes factor in favor of the common-spectrum process versus independent red-noise processes in each pulsar exceeds $10,000$. However, we find no statistically significant evidence that this process has quadrupolar spatial correlations, which we would consider necessary to claim a GWB detection consistent with General Relativity. We find that the process has neither monopolar nor dipolar correlations, which may arise from, for example, reference clock or solar-system ephemeris systematics, respectively. The amplitude posterior has significant support above previously reported upper limits; we explain this in terms of the Bayesian priors assumed for intrinsic pulsar red noise. We examine potential implications for the supermassive black hole binary population under the hypothesis that the signal is indeed astrophysical in nature.

$$\Omega_{\rm GW} h^2 = \frac{2\pi^2}{3} h_c^2 \left(\frac{f_{\rm yr}}{100\,{\rm km\,s^{-1}\,Mpc^{-1}}} \right)^2 \simeq 2.3 \times 10^{-9}$$

Supported by PPTA
arXiv:2107.12112

Gravitational Waves

$$h_{ij}(t,\boldsymbol{x}) = \sum_{P=+,\times} \int_{-\infty}^{\infty} df \int_{S^2} d\boldsymbol{n} h_P(f,\boldsymbol{n}) e^{2\pi i f(-t+\boldsymbol{n}\cdot\boldsymbol{x})} e^P_{ij}(\boldsymbol{n}). \quad (1)$$

Here, the bases for transverse-traceless tensor e^P ($P = +, \times$) are given as

$$e^+ = \hat{e}_\theta \otimes \hat{e}_\theta - \hat{e}_\phi \otimes \hat{e}_\phi, \qquad e^\times = \hat{e}_\theta \otimes \hat{e}_\phi + \hat{e}_\phi \otimes \hat{e}_\theta,$$

$$\begin{pmatrix} \langle h_+(f,\boldsymbol{n}) h_+^*(f',\boldsymbol{n}')\rangle & \langle h_+(f,\boldsymbol{n}) h_\times^*(f',\boldsymbol{n}')\rangle \\ \langle h_\times(f,\boldsymbol{n}) h_+^*(f',\boldsymbol{n}')\rangle & \langle h_\times(f,\boldsymbol{n}) h_\times^*(f',\boldsymbol{n}')\rangle \end{pmatrix}$$

$$= \frac{1}{2}\delta_{\mathrm{D}}^2(\boldsymbol{n}-\boldsymbol{n}')\delta_{\mathrm{D}}(f-f') \times \begin{pmatrix} I(f,\boldsymbol{n}) + Q(f,\boldsymbol{n}) & U(f,\boldsymbol{n}) - iV(f,\boldsymbol{n}) \\ U(f,\boldsymbol{n}) + iV(f,\boldsymbol{n}) & I(f,\boldsymbol{n}) - Q(f,\boldsymbol{n}) \end{pmatrix}.$$

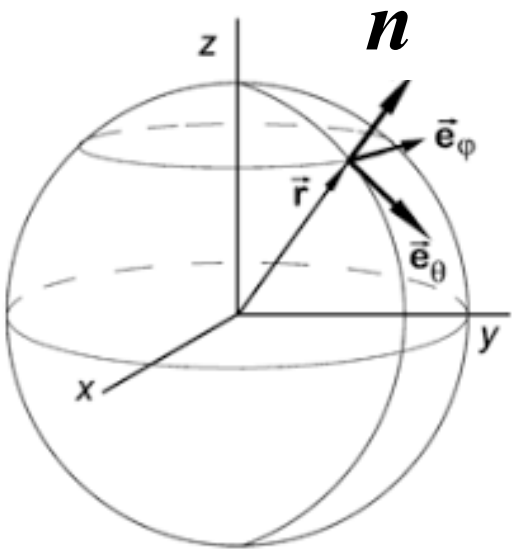

Q= <++> - <xx>
U is the same as in a frame rotated by π/8

$$e^R = \frac{(e^+ + ie^\times)}{\sqrt{2}}, \qquad e^L = \frac{(e^+ - ie^\times)}{\sqrt{2}}$$

$$h_R = \frac{(h_+ - ih_\times)}{\sqrt{2}}, \qquad h_L = \frac{(h_+ + ih_\times)}{\sqrt{2}}$$

$$\begin{pmatrix} \langle h_R(f,\boldsymbol{n}) h_R(f',\boldsymbol{n}')^*\rangle & \langle h_L(f,\boldsymbol{n}) h_R(f',\boldsymbol{n}')^*\rangle \\ \langle h_R(f,\boldsymbol{n}) h_L(f',\boldsymbol{n}')^*\rangle & \langle h_L(f,\boldsymbol{n}) h_L(f',\boldsymbol{n}')^*\rangle \end{pmatrix}$$

$$= \frac{1}{2}\delta_{\mathrm{D}}(\boldsymbol{n}-\boldsymbol{n}')^2\delta_{\mathrm{D}}(f-f') \times \begin{pmatrix} I(f,\boldsymbol{n}) + V(f,\boldsymbol{n}) & Q(f,\boldsymbol{n}) - iU(f,\boldsymbol{n}) \\ Q(f,\boldsymbol{n}) + iU(f,\boldsymbol{n}) & I(f,\boldsymbol{n}) - V(f,\boldsymbol{n}) \end{pmatrix}.$$

GWB Anisotropy and Polarization Angular Power Spectra

Decompose the GWB sky into a sum of spherical harmonics:

$$T(\theta,\varphi) = \Sigma_{lm}\ a_{lm}\ Y_{lm}\ (\theta,\varphi),\quad V(\theta,\varphi) = \Sigma_{lm}\ b_{lm}\ Y_{lm}\ (\theta,\varphi)$$

$$(Q - iU)\ (\theta,\varphi) = \Sigma_{lm}\ a_{4,lm}\ {}_4Y_{lm}\ (\theta,\varphi)$$

$$(Q + iU)\ (\theta,\varphi) = \Sigma_{lm}\ a_{-4,lm}\ {}_{-4}Y_{lm}\ (\theta,\varphi)$$

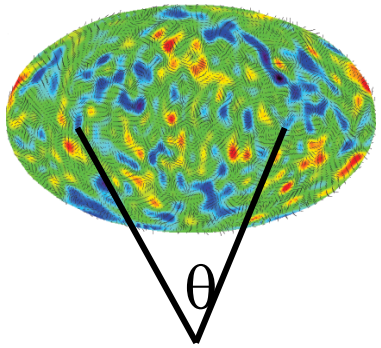

l = 180 degrees/ θ

$C^T_l = \Sigma_m\ (a^*_{lm}\ a_{lm})$ anisotropy power spectrum

$C^V_l = \Sigma_m\ (b^*_{lm}\ b_{lm})$ circular polarization power spectrum

$C^E_l = \Sigma_m\ (a^*_{4,lm}\ a_{4,lm} + a^*_{4,lm}\ a_{-4,lm})$ E-polarization power spectrum

$C^B_l = \Sigma_m\ (a^*_{4,lm}\ a_{4,lm} - a^*_{4,lm}\ a_{-4,lm})$ B-polarization power spectrum

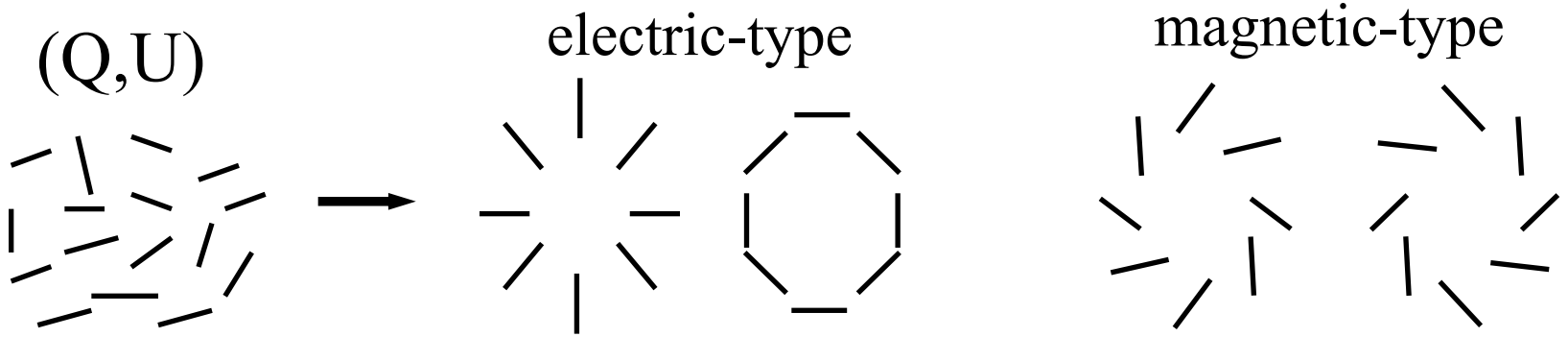

GWB Anisotropy from the Sachs-Wolfe Effect

Collisionless Boltzman Equation for Gravitons e.g. Bartolo et al. 19

$$ds^2 = a^2(\eta)\left[-e^{2\Phi}d\eta^2 + (e^{-2\Psi}\delta_{ij} + h_{ij})dx^i dx^j\right]$$

$$\frac{\partial f}{\partial \eta} + \frac{\partial f}{\partial x^i}\frac{dx^i}{d\eta} + \frac{\partial f}{\partial q}\frac{dq}{d\eta} + \frac{\partial f}{\partial n^i}\frac{dn^i}{d\eta} = 0$$

Graviton phase space distribution function

$$f = f(\eta, x^i, q, \hat{n}^i)$$

$$\frac{\partial f}{\partial \eta} + n^i \frac{\partial f}{\partial x^i} + \left[\frac{\partial \Psi}{\partial \eta} - n^i \frac{\partial \Phi}{\partial x^i} + \frac{1}{2} n^i n^j \frac{\partial h_{ij}}{\partial \eta}\right] q \frac{\partial f}{\partial q} = 0$$

$$\delta f \equiv -q \frac{\partial \bar{f}}{\partial q} \Gamma(\eta, \vec{x}, q, \hat{n})$$

k-mode $\Gamma(\eta, \vec{x}, q, \hat{n}) = \int \frac{d^3k}{(2\pi)^3} \Gamma(\eta, \vec{k}, q, \hat{n}) e^{i\vec{k}\cdot\vec{x}}$

Newtonian potential k-mode

$$\Psi = \Phi \equiv T_\Phi(\eta, k)\,\hat{\zeta}(\vec{k})$$

Transfer function

Initial scalar (density) power spectrum

GW background k-mode

$$h_{ij} \equiv \sum_{\lambda=\pm 2} e_{ij,\lambda}(\hat{k}) h(\eta, k) \hat{\xi}_\lambda(k^i)$$

Transfer function

Initial tensor power spectrum

$$\Gamma(\hat{n}) = \sum_\ell \sum_{m=-\ell}^{\ell} \Gamma_{\ell m} Y_{\ell m}(\hat{n}) \qquad e^{i\vec{k}\cdot\vec{x}} = 4\pi \sum_{lm} i^l j_l(kx) Y^*_{lm}(\hat{k}) Y_{lm}(\hat{x})$$

Scalar contribution

$$\frac{\Gamma_{\ell m,S}}{4\pi\,(-i)^\ell} = \int \frac{d^3k}{(2\pi)^3}\,\zeta(\vec{k}) Y^*_{\ell m}(\hat{k})\,\mathcal{T}^{(0)}_\ell(k,\,\eta_0,\,\eta_{\rm in})$$

$\vec{x}_0 = 0$
η_0 today
$\eta_{\rm in}$ initial

$T_\Phi(\eta_{\rm in}, k) = 3/5$

where the scalar transfer function $\mathcal{T}^{(0)}_\ell$ is the sum of a term analogous to the SW effect for CMB photons, $T_\Phi(\eta_{\rm in}, k)\, j_\ell[k(\eta_0 - \eta_{\rm in})]$, plus the analog of the ISW term, $\int_{\eta_{\rm in}}^{\eta_0} d\eta' \,[T'_\Psi(\eta, k) + T'_\Phi(\eta, k)]\, j_\ell[k(\eta - \eta_{\rm in})]$. Finally,

Tensor contribution

$$\mathcal{T}^{(\pm 2)}_\ell = \frac{1}{4}\sqrt{\frac{(\ell+2)!}{(\ell-2)!}} \int_{\eta_{\rm in}}^{\eta_0} d\eta\, h'(\eta,\,k)\, \frac{j_\ell\,[k\,(\eta_0 - \eta)]}{k^2\,(\eta_0 - \eta)^2}$$

Sachs-Wolfe or Integrated Sachs-Wolfe effects – gravitational redshift of gravitons

GWB Anisotropy Map due to SW and ISW Effects

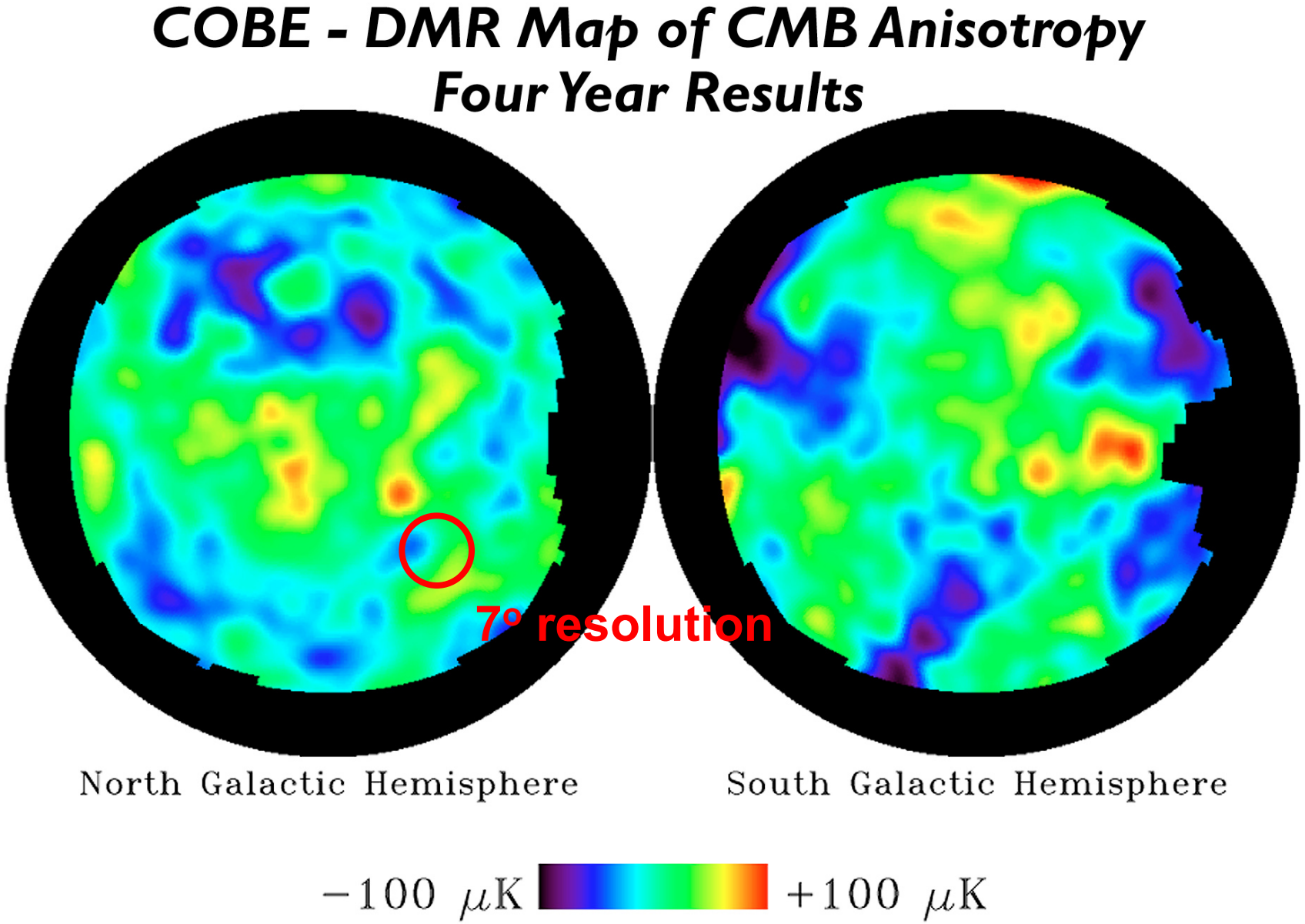

GWB Anisotropy from Primordial Black-Hole Seeds

Primordial black-hole seeds or density (scalar) perturbation associated GWs

$$\left[\frac{\partial^2}{\partial\eta^2}+\frac{2}{a}\frac{da}{d\eta}\frac{\partial}{\partial\eta}-\vec{\nabla}^2\right]h_{ij}=0$$

Free gravitational wave equation

De Sitter vacuum fluctuations during inflation lead to almost scale-invariant primordial gravitational waves

$P_h = 8\pi GH^2$ and $\Delta_\zeta^2 = \langle\zeta\zeta\rangle = (\delta\rho/\rho)^2 \sim 2\times10^{-9}$ on CMB scales

$$\left[\frac{\partial^2}{\partial\eta^2}+\frac{2}{a}\frac{da}{d\eta}\frac{\partial}{\partial\eta}-\vec{\nabla}^2\right]h_{ij}=16\pi G T_{ij}$$

Stress due to transverse traceless part of 2nd order curvature perturbation $T_{ij}(\zeta^2)$

$\Delta_\zeta^2 = \langle\zeta\zeta\rangle = (\delta\rho/\rho)^2 \sim 10^{-3}$

When large density perturbation re-enter the horizon during the radiation-dominated era and collapse to form PBHs, they induce gravitational waves at short wavelengths

Ananda, Clarkson,Wands 2007, Baumann, Steinhardt,Takahashi,Ichiki 2007

Production of PBH seeds in axion monodromy inflation with sinusoidal modulations

$M_{BH}\sim 10^{8}$ g

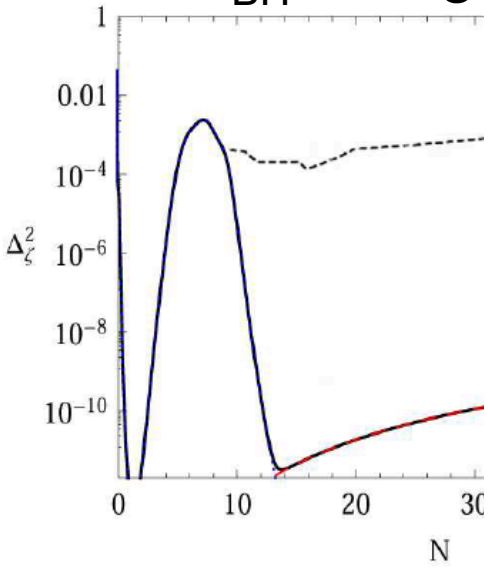

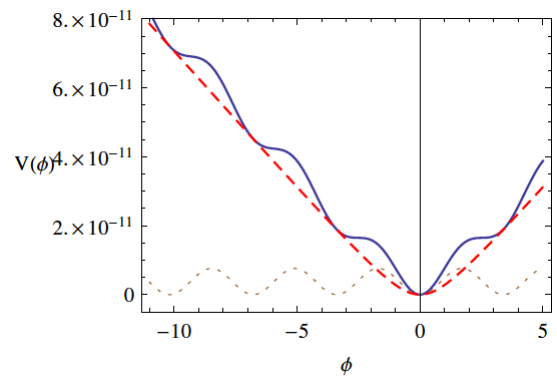

$M_{BH}\sim 10^{-13}M_\odot$

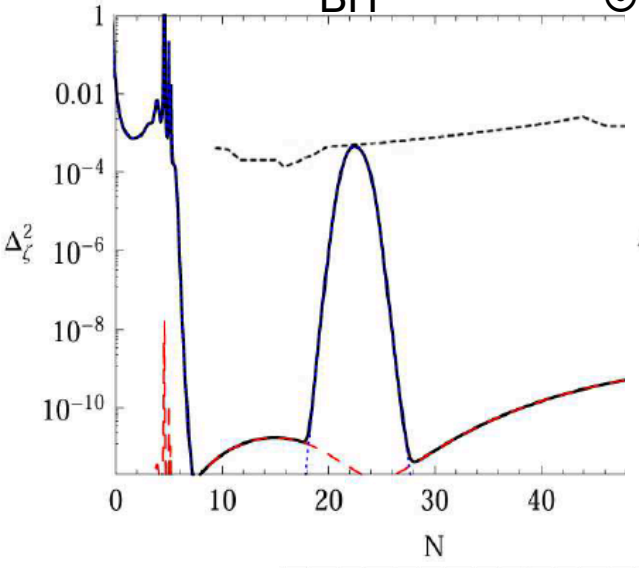

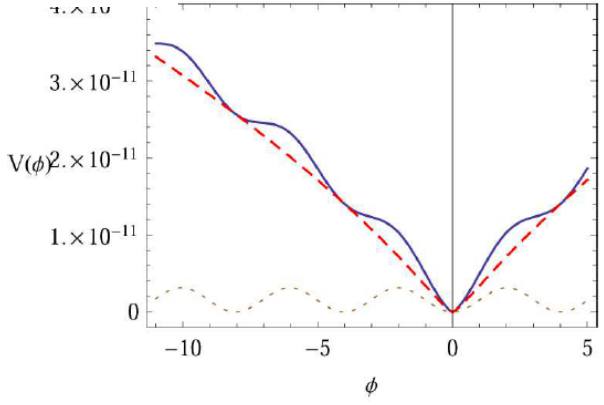

$M_{BH}\sim 20M_\odot$

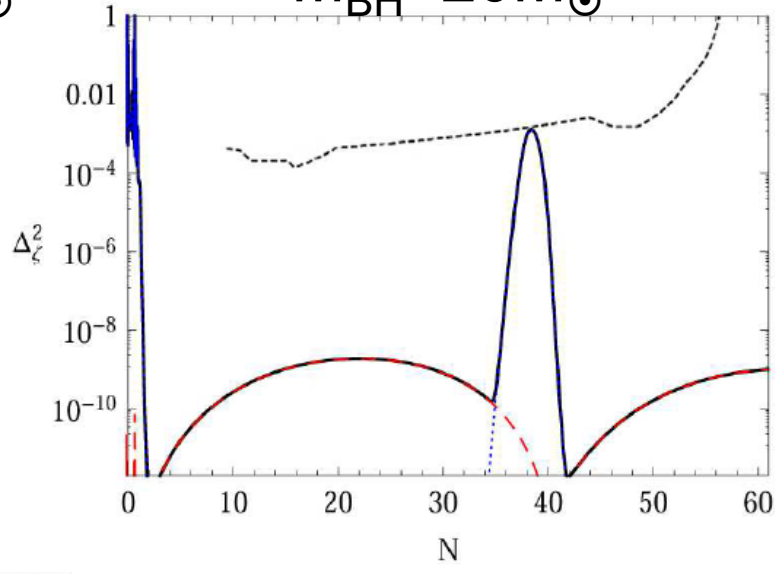

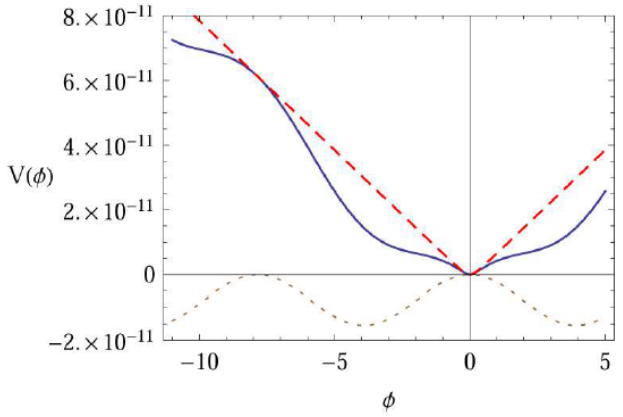

GWs associated with PBHs in modulated axion inflation

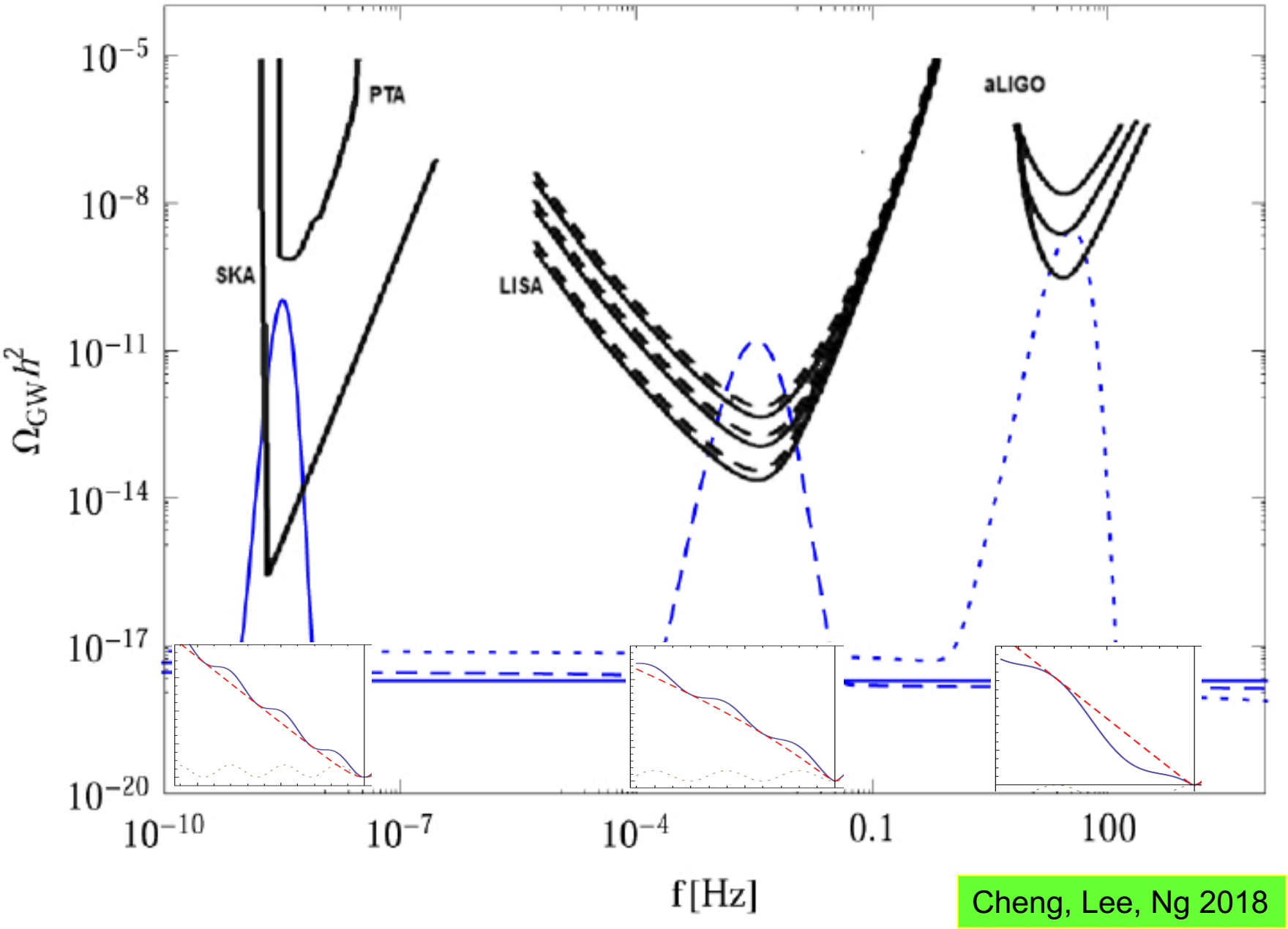

Cheng, Lee, Ng 2018

Non-gaussian density perturbations

Newtonian potential

$$\Phi(\vec{x}) = \phi(\vec{x}) + f_{NL}\left(\phi(\vec{x})^2 - \langle\phi(\vec{x})^2\rangle\right)$$

$$\phi(\vec{x}) = \int \frac{d^3\vec{k}}{(2\pi)^{\frac{3}{2}}}\phi(\vec{k})e^{i\vec{k}\cdot\vec{x}},$$

$$\langle\phi(\vec{k})\phi^*(\vec{k'})\rangle = \delta(\vec{k}-\vec{k'})P_\phi(k).$$

$$\langle\Phi\left(\vec{x}+\vec{r}/2\right)\Phi\left(\vec{x}-\vec{r}/2\right)\rangle_{\text{subvolume}} = \int_{|\vec{k}|>k_{\min}} \frac{d^3\vec{k}}{(2\pi)^3}e^{i\vec{k}\cdot\vec{r}}P_\phi(k)\left[1+4f_{NL}\int_{|\vec{p}|<k_{\min}} \frac{d^3\vec{p}}{(2\pi)^{\frac{3}{2}}}\phi(\vec{p})\cos\left(\frac{\vec{p}\cdot\vec{r}}{2}\right)e^{i\vec{p}\cdot\vec{x}}\right].$$

subvolume = observable universe

For $\vec{p}\cdot\vec{r} \ll 1$, we have the position dependent power spectrum,

$$P_\Phi(k,\vec{x}) \simeq P_\phi(k)\left[1+4f_{NL}\int_{|\vec{p}|<k_{\min}} \frac{d^3\vec{p}}{(2\pi)^{\frac{3}{2}}}\phi(\vec{p})e^{i\vec{p}\cdot\vec{x}}\right].$$

Induced GW power spectrum

$$P_h(k,\vec{x}) \simeq P_h(k)\left[1+8f_{NL}\int_{|\vec{p}|<k_{\rm min}}\frac{d^3\vec{p}}{(2\pi)^{\frac{3}{2}}}\phi(\vec{p})e^{i\vec{p}\cdot\vec{x}}\right], \quad (15)$$

so the observed spectrum is given by $P_h(k,\hat{k}) = P_h(k,x_h\hat{k})$, where $x = x_h$ is the comoving distance to the horizon re-entry and $k_{\rm min} = \pi/x_h$. Let us expand

$$P_h(k,\hat{k}) \simeq P_h(k)\left[1+f_{NL}\sum_{lm}a_{lm}Y_{lm}(\hat{k})\right],$$

$$a_{lm} = 32\pi i^l\int_{|\vec{p}|<k_{\rm min}}\frac{d^3\vec{p}}{(2\pi)^{\frac{3}{2}}}j_l(px_h)\phi(\vec{p})Y^*_{lm}(\hat{p}). \quad (16)$$

$$x_h = \eta_0 - \eta_c \simeq \eta_0$$

which is the superhorizon-mode contribution ($p\eta_0 < \pi$) of the SW effect

Planck data: $-40 < f_{NL} < 40$ $\quad l < 100$

Implication

- Non-Gaussian super-horizon-mode perturbations have been used to explain the large-scale CMB anomalies
- Anisotropy in GWB may give an independent evidence of the non-Gaussianity

WMAP3
CMB sky map

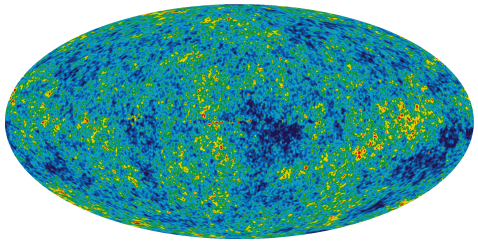

$$\delta T(\theta,\phi) = \sum_{l,m} a_{lm} Y_{lm}(\theta,\phi)$$

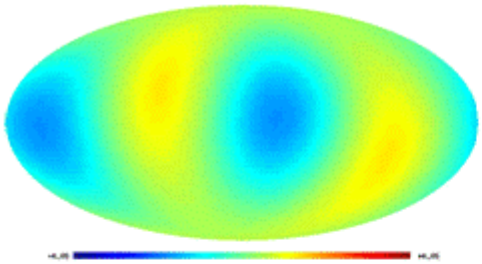

$\ell = 2$

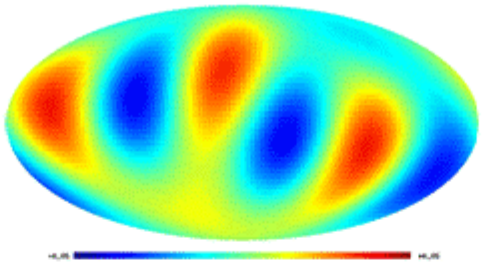

$\ell = 3$

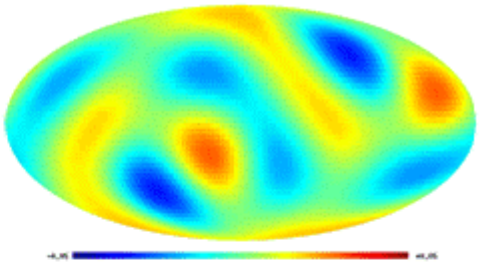

$\ell = 4$

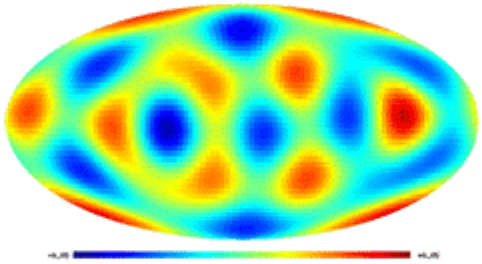

$\ell = 5$

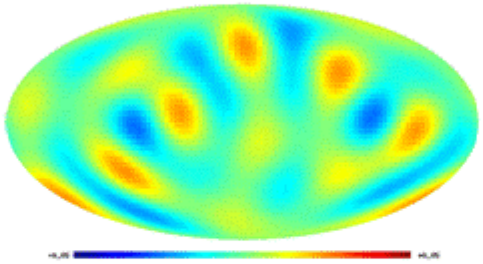

$\ell = 6$

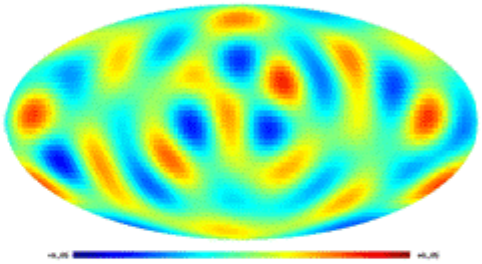

$\ell = 7$

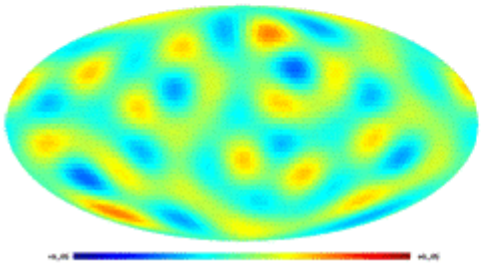

$\ell = 8$

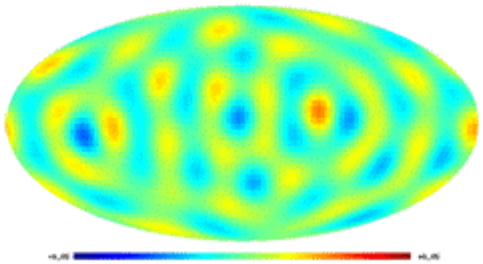

$\ell = 9$

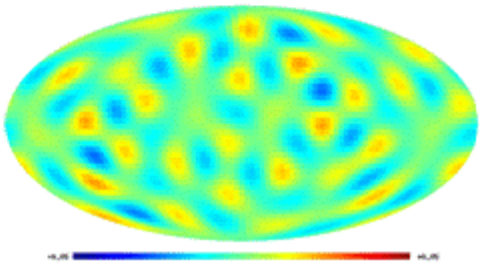

$\ell = 10$

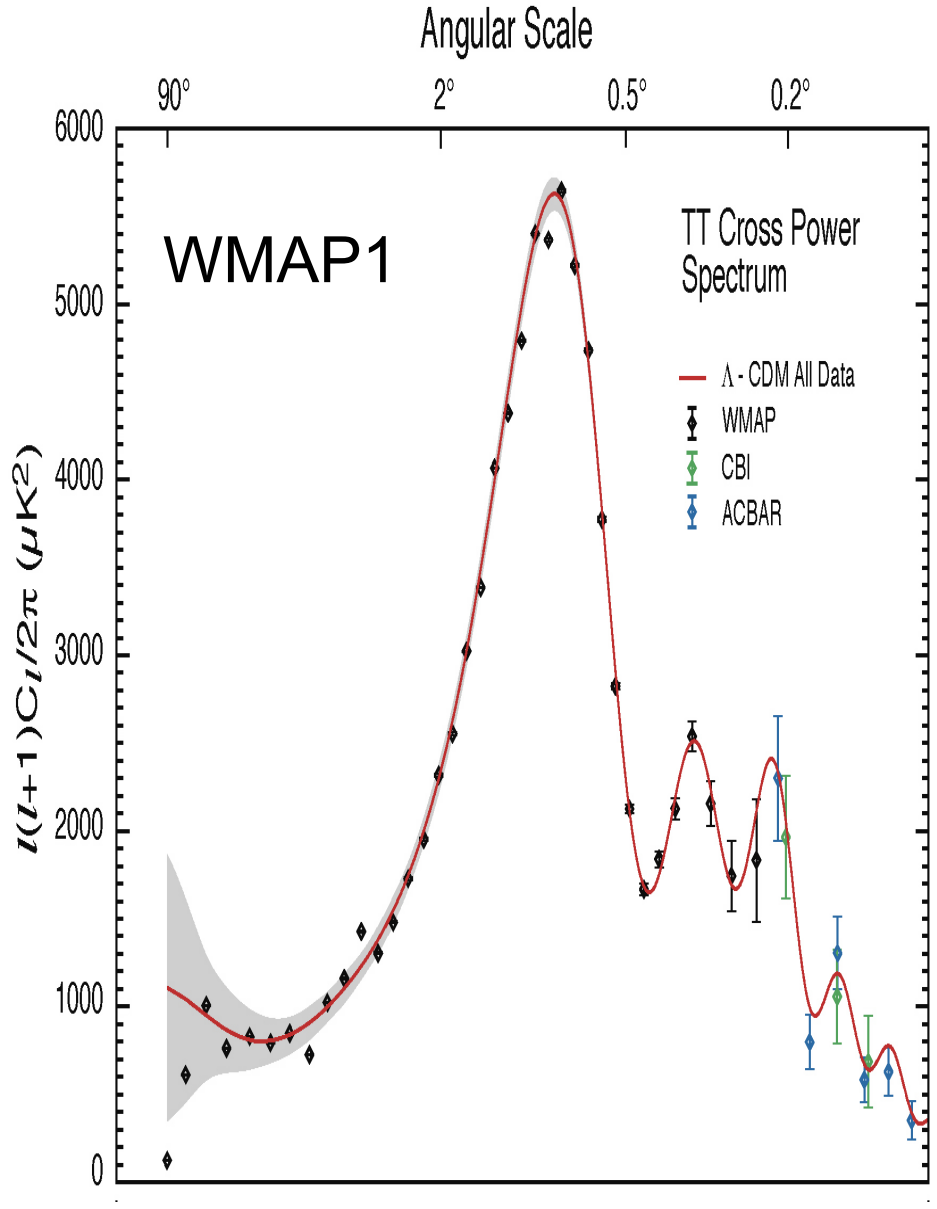
Angular Scale
90°
2°
0.5°
0.2°
WMAP1
TT Cross Power Spectrum
Λ - CDM All Data
WMAP
CBI
ACBAR
l(l+1)Cl/2π (μK2)
6000
5000
4000
3000
2000
1000
0

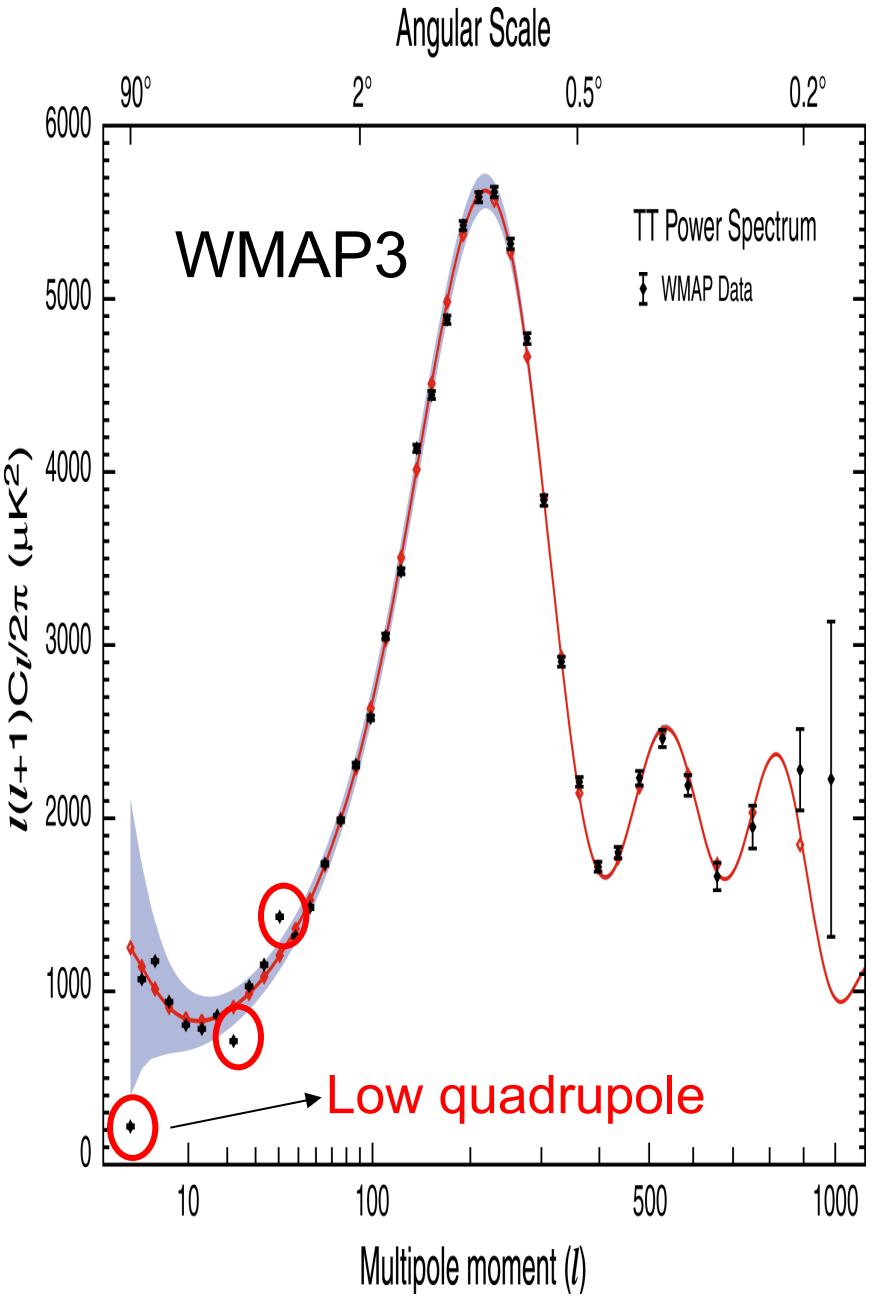
Angular Scale
90°
2°
0.5°
0.2°
WMAP3
TT Power Spectrum
WMAP Data
Low quadrupole
l(l+1)Cl/2π (μK2)
6000
5000
4000
3000
2000
1000
0
10
100
500
1000
Multipole moment (l)

South-North Power Asymmetry

Eriksen et al 04
Park 04

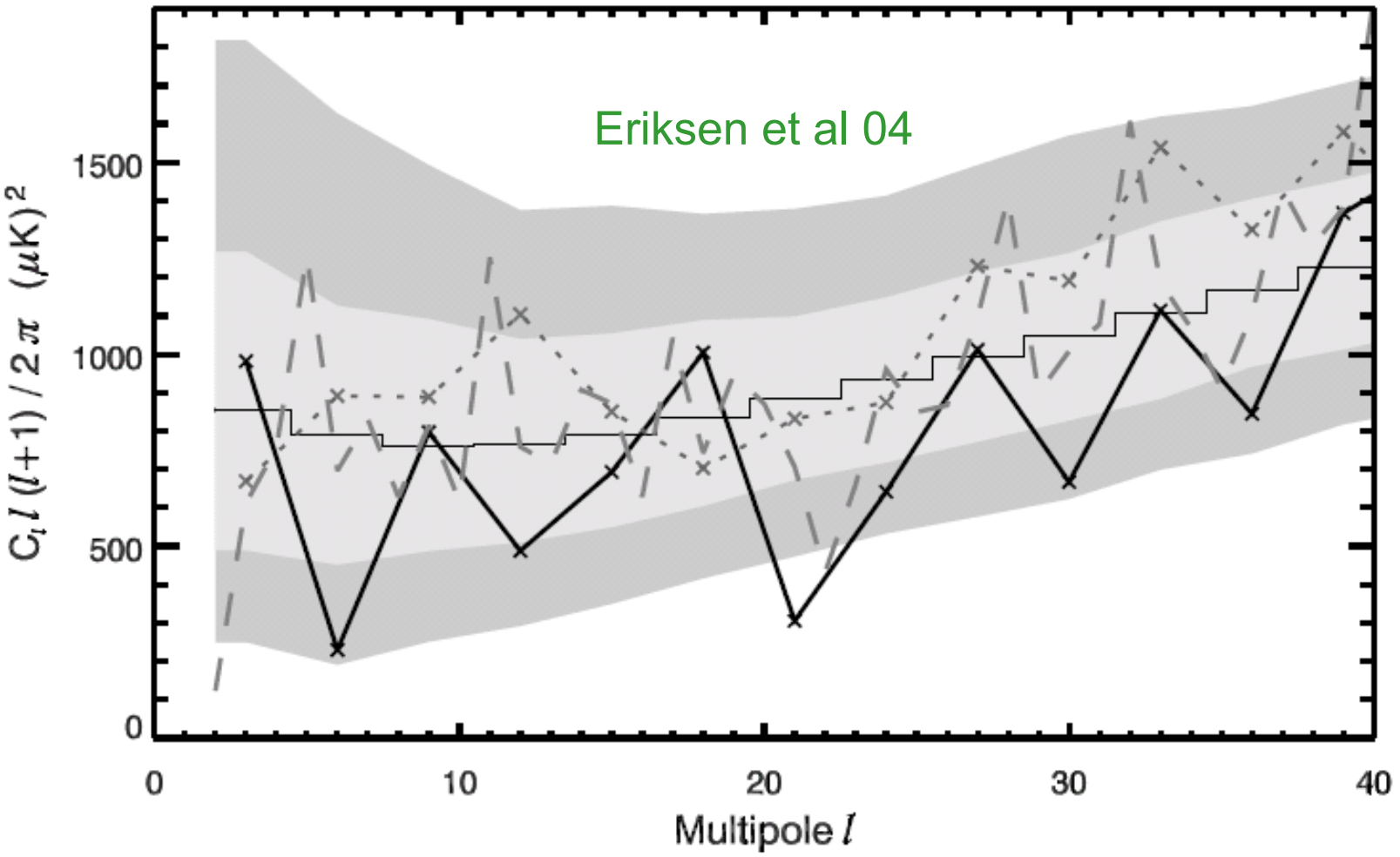

northern hemisphere
southern hemisphere
full sky

North pole (80°,57°)

Land & Magueijo 05

"Axis of Evil" $(l,b)\sim(-110°,60°)$

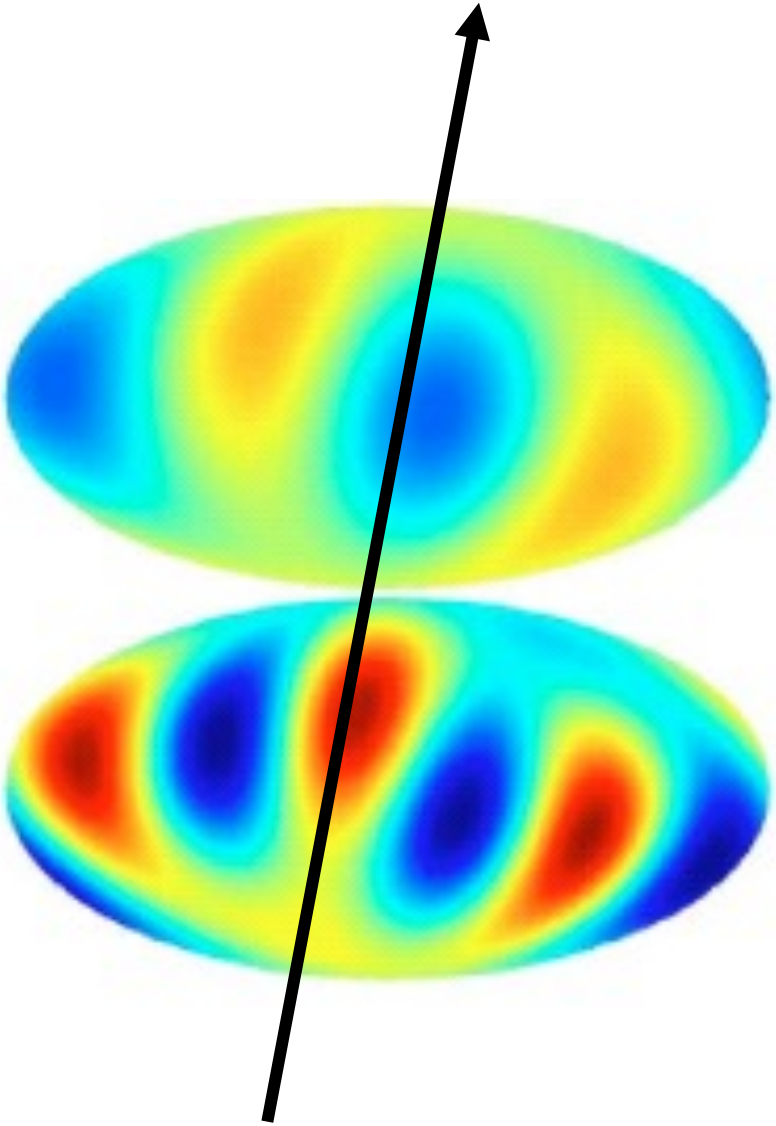

l=2, quadrupole

l=3, octopole

GWB Circular Polarization

$$\left[\frac{\partial^2}{\partial\eta^2}+\frac{2}{a}\frac{da}{d\eta}\frac{\partial}{\partial\eta}-\vec{\nabla}^2\right]h_{ij}=16\pi G T_{ij}$$

Stress due to transverse traceless part of 2nd order curvature perturbation $T_{ij}(\zeta^2)$

$\Delta_\zeta^2 = \langle\zeta\zeta\rangle = (\delta\rho/\rho)^2 \sim 10^{-3}$

In axion inflation, the coupling of the axion to photon can produce helical photons T_{ij}

$$\left[\frac{\partial^2}{\partial\eta^2}+\frac{2}{a}\frac{da}{d\eta}\frac{\partial}{\partial\eta}-\vec{\nabla}^2\right]h_{ij}=\frac{2a^2}{M_p^2}\left(-E_iE_j-B_iB_j\right)^{TT}$$

Transverse traceless part of photon energy-momentum

$\langle E\cdot E\rangle \sim \langle E\cdot B\rangle \sim \zeta$

These helical photons source circularly polarized GWs

Overlap Reduction Functions (ORFs) – Reponses of detectors to GWs

GW observables

The method adopted in current GW experiments for detecting SGWB is to correlate responses of different detectors to the GW strain amplitude. This allows us to filter out detector noises and obtain a large signal-to-noise ratio [4]. Let $h(\vec{x})$ be the response of a detector located at $\vec{x}$ with a pair of arms d_{ij}; then, we have

$$h(\vec{x}) \equiv d^{ij} h_{ij}(\vec{x}) = \sum_{\lambda=+,\times} \int \frac{d^3\vec{k}}{(2\pi)^{\frac{3}{2}}} h_\lambda(\vec{k}) F^\lambda(\hat{k}) e^{i\vec{k}\cdot\vec{x}}, \tag{6}$$

where $F^\lambda = d^{ij}\epsilon^\lambda_{ij}(\hat{k})$ is the beam-pattern function. Hence, using Eq. (3) the response correlation between two detectors a and b, located at $\vec{x}_a = \vec{x} + \vec{r}/2$ and $\vec{x}_b = \vec{x} - \vec{r}/2$ respectively, is given by

$$\langle h_a(\vec{x}_a) h_b(\vec{x}_b)\rangle = \sum_{\lambda=+,\times} \int \frac{d^3\vec{k}}{(2\pi)^3} P_h(k) F^\lambda_a(\hat{k}) F^\lambda_b(\hat{k}) e^{i\vec{k}\cdot\vec{r}}, \tag{7}$$

GW power spectrum

$$P_h(k) \equiv (2\pi^2/k^3)\mathcal{P}_h(k)$$

Current Pulsar Timing Arrays (PTAs)

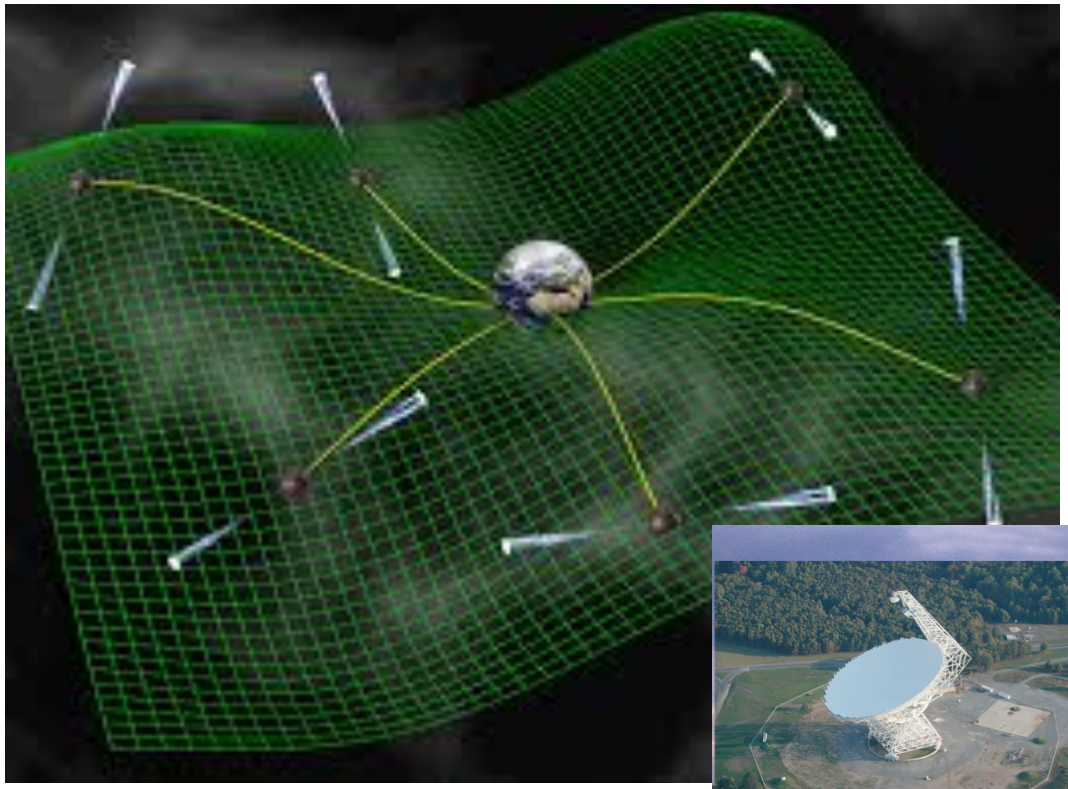

Nano-Hz GWs cause small correlated changes to the times of arrival of radio pulses from millisecond pulsars (MSPs)

International Pulsar Timing Arrays

Pulsar Timing – MSPs are precise clocks

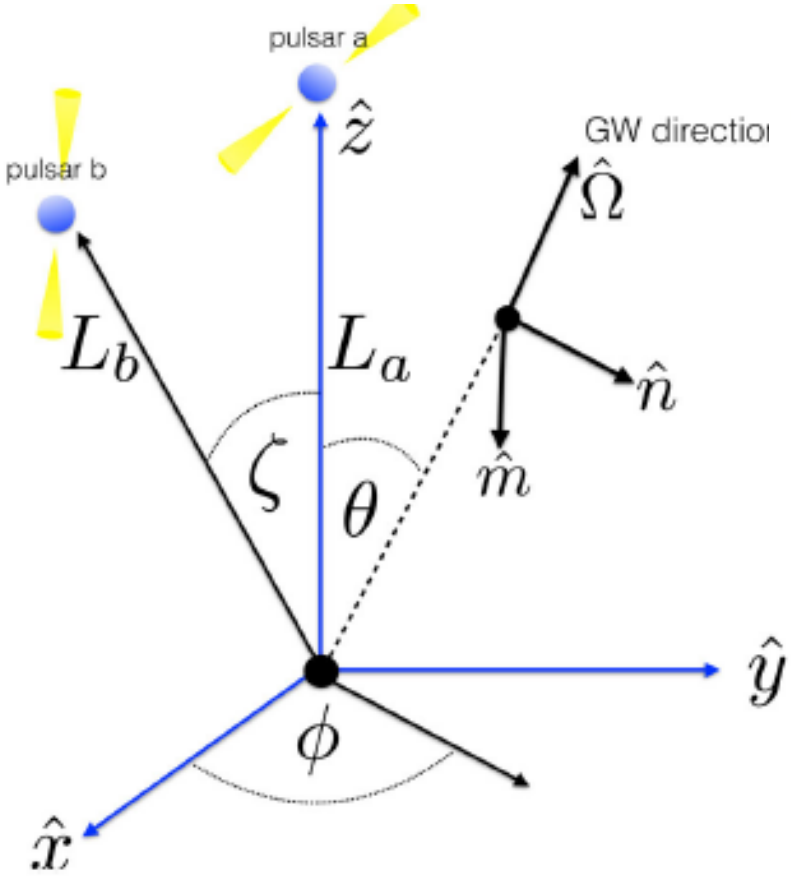

$$z(t,\hat{\Omega}) \equiv \frac{\nu(t)-\nu_0}{\nu_0} = \frac{1}{2}\frac{\hat{p}^i\hat{p}^j}{1+\hat{\Omega}\cdot\hat{p}}\Delta h_{ij}(t,\hat{\Omega}),$$

Shapiro time delay

$$\Delta h_{ij}(t,\hat{\Omega}) \equiv h_{ij}(t,\hat{\Omega}) - h_{ij}(t_p,\hat{\Omega})$$

$$z(t) = \int d\hat{\Omega} z(t,\hat{\Omega})$$

pulsar residual $\quad r(t) = \int^t dt' z(t')$

detector tensor

$d^{ij} = p^i p^j$

$$\langle r_a^*(t_j) r_b(t_k)\rangle = \left\langle \int^{t_j} dt' \int^{t_k} dt'' z_a^*(t') z_b(t'')\right\rangle$$

$$\langle r_a^*(t_j) r_b(t_k) \rangle = \int^{t_j} dt' \int^{t_k} dt'' \int_{-\infty}^{+\infty} df e^{-i2\pi f(t'-t'')} H(f)^{(ab)}\Gamma(f)$$

$$\langle h_A^*(f,\hat{\Omega}) h_{A'}(f',\hat{\Omega}') \rangle = \delta^2(\hat{\Omega},\hat{\Omega}')\delta_{AA'}\delta(f-f')H(f)P(\hat{\Omega})$$

Overlap Reduction Function

$$^{(ab)}\Gamma(f) \equiv \int d\hat{\Omega} P(\hat{\Omega}) \kappa_{ab}(f,\hat{\Omega}) \left[\sum_A F_a^A(\hat{\Omega}) F_b^A(\hat{\Omega}) \right],$$

$$\kappa_{ab}(f,\hat{\Omega}) \equiv [1 - e^{i2\pi f L_a(1+\hat{\Omega}\cdot\hat{p}_a)}][1 - e^{-i2\pi f L_b(1+\hat{\Omega}\cdot\hat{p}_b)}], \qquad F^A(\hat{\Omega}) = \left[\frac{1}{2} \frac{\hat{p}^i \hat{p}^j}{1+\hat{\Omega}\cdot\hat{p}} e_{ij}^A(\hat{\Omega}) \right]$$

Earth term

pulsar term $fL >> 1$

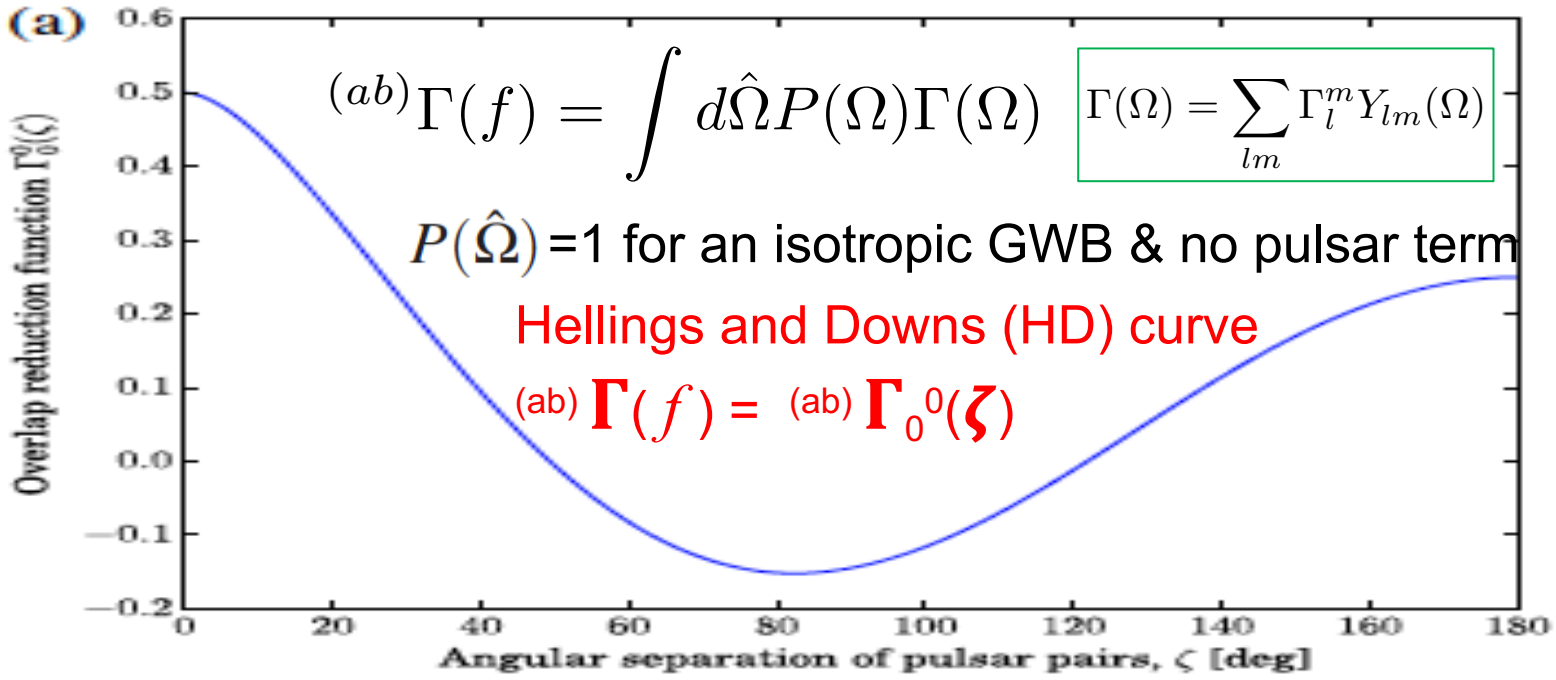

$$^{(ab)}\Gamma(f) = \int d\hat{\Omega} P(\Omega)\Gamma(\Omega) \qquad \Gamma(\Omega) = \sum_{lm} \Gamma_l^m Y_{lm}(\Omega)$$

$P(\hat{\Omega})$ =1 for an isotropic GWB & no pulsar term

Hellings and Downs (HD) curve

$^{(ab)}\boldsymbol{\Gamma}(f) = {}^{(ab)}\boldsymbol{\Gamma}_0^0(\boldsymbol{\zeta})$

We have developed an efficient tool for generating ORF spherical harmonics $\Gamma_{lm}(f)$ for LIGO-Virgo-KAGRA detector pair

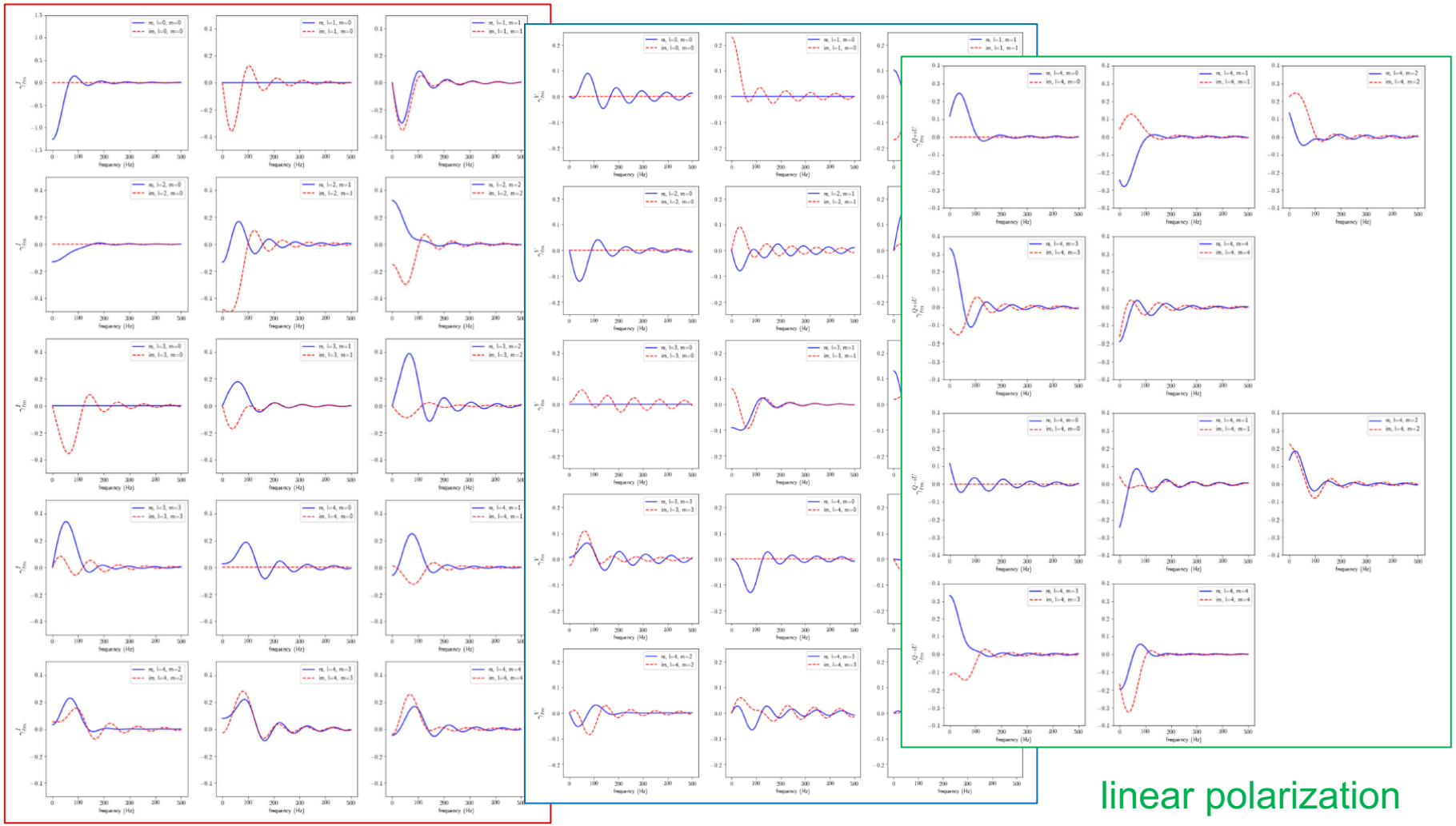

anisotropy

circular polarization

linear polarization

Chu+Liu+Ng 21

We have developed an efficient tool for generating ORF $\mathbf{\Gamma}_{lm}(\zeta)$ for any pulsar pair with separation angle ζ

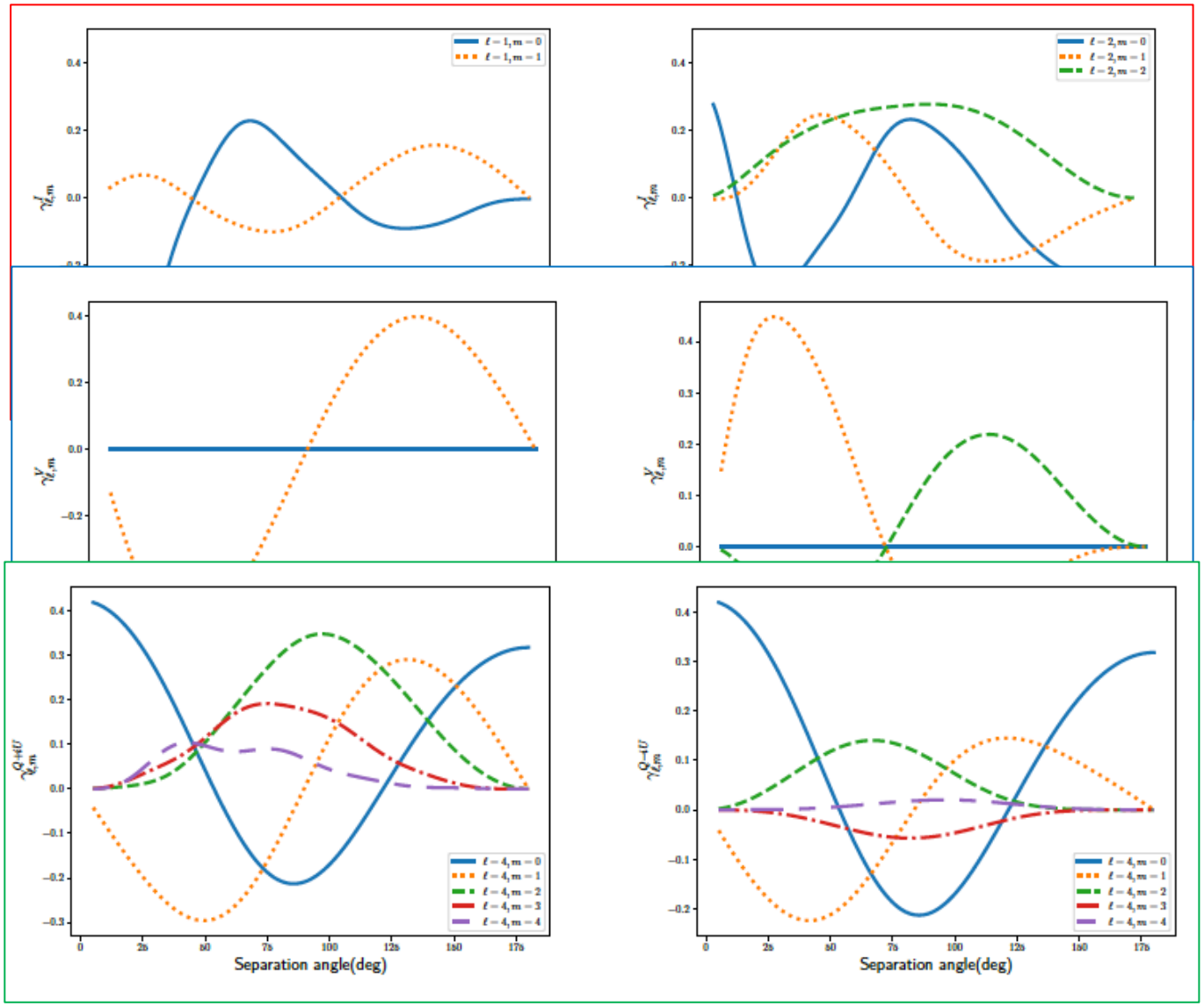

anisotropy

circular polarization

linear polarization

Perspectives
(personal viewpoints)

Future GW direct experiments

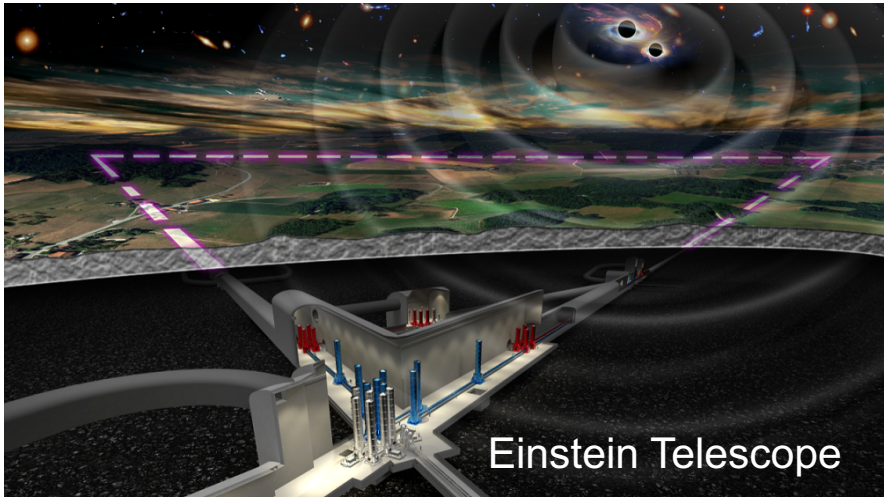

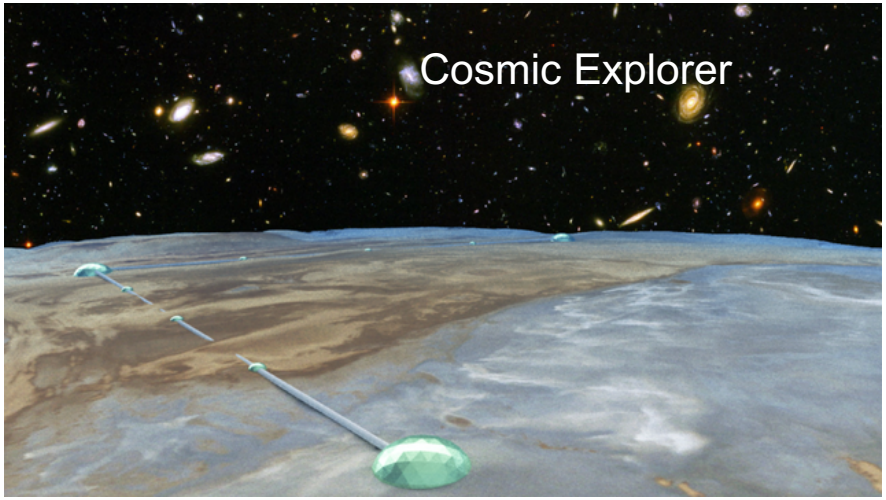

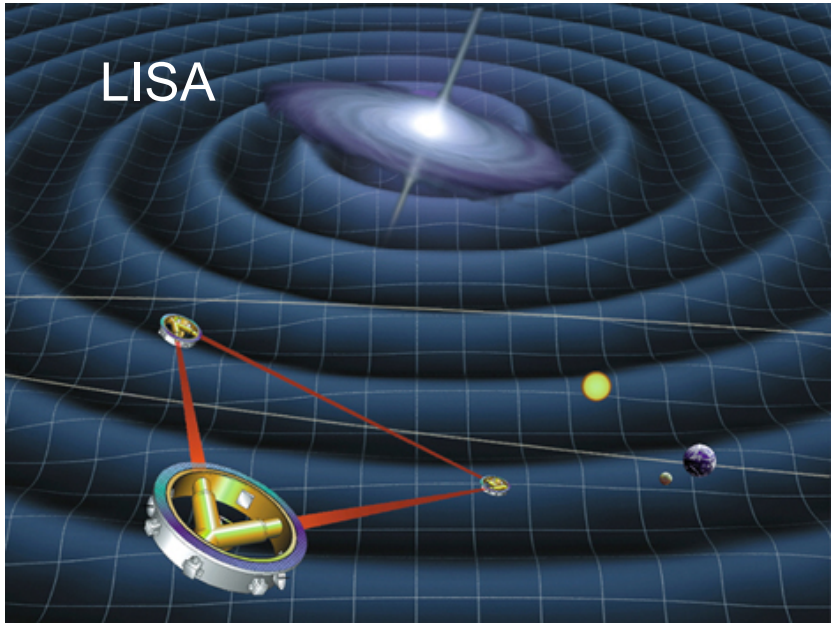

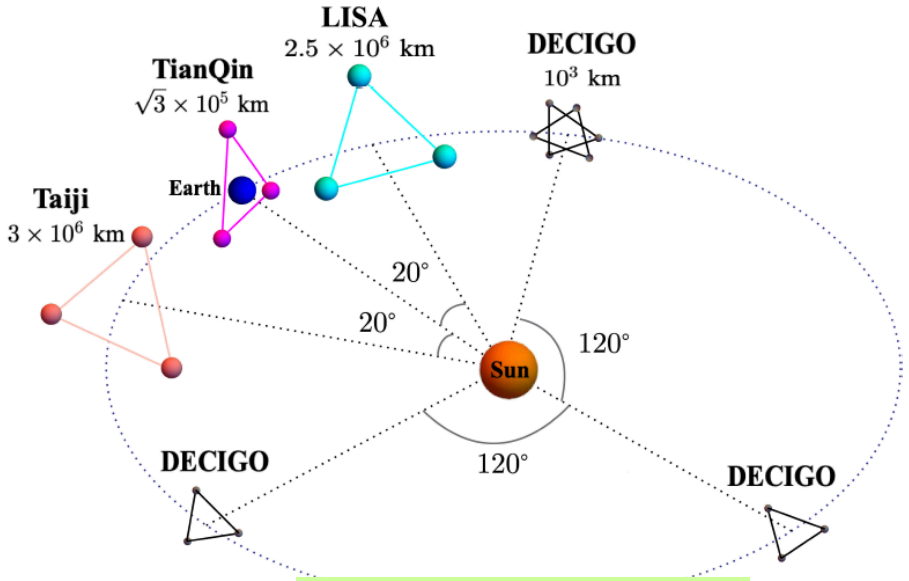

GW space network

Current Pulsar Timing Arrays

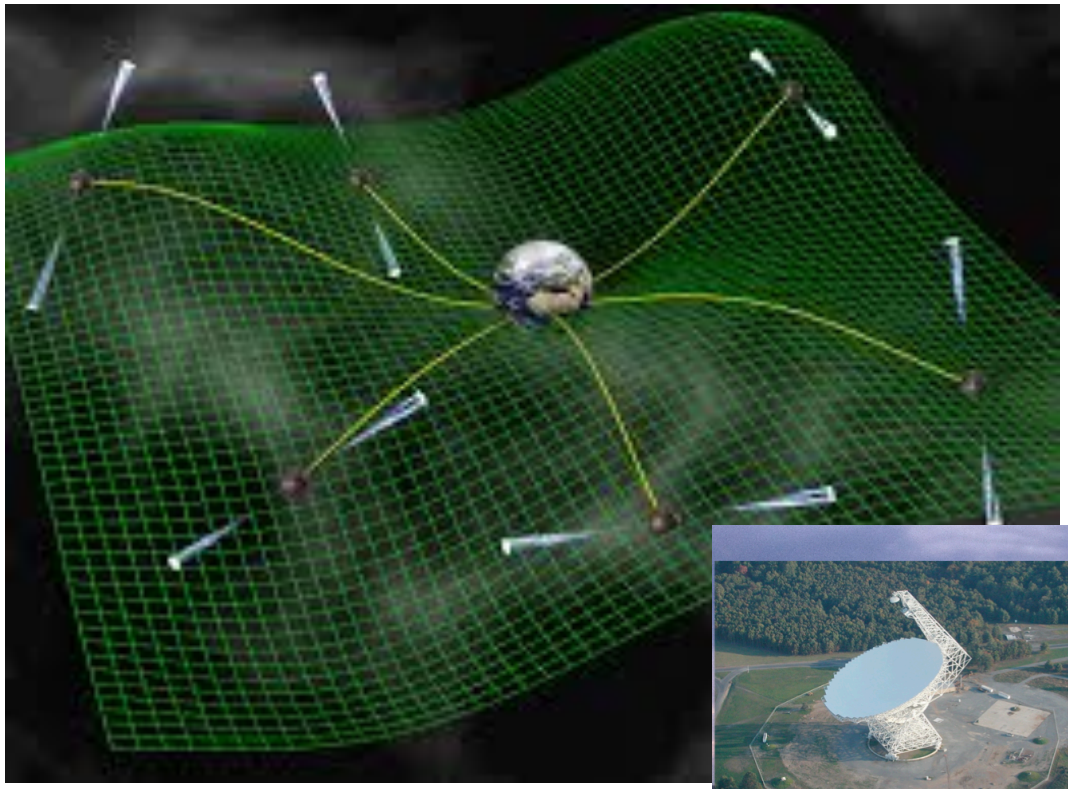

Nano-Hz GWs cause small correlated changes to the times of arrival of radio pulses from millisecond pulsars (MSPs)

International Pulsar Timing Arrays

The NANOGrav 12.5 year data set: 45 MSPs

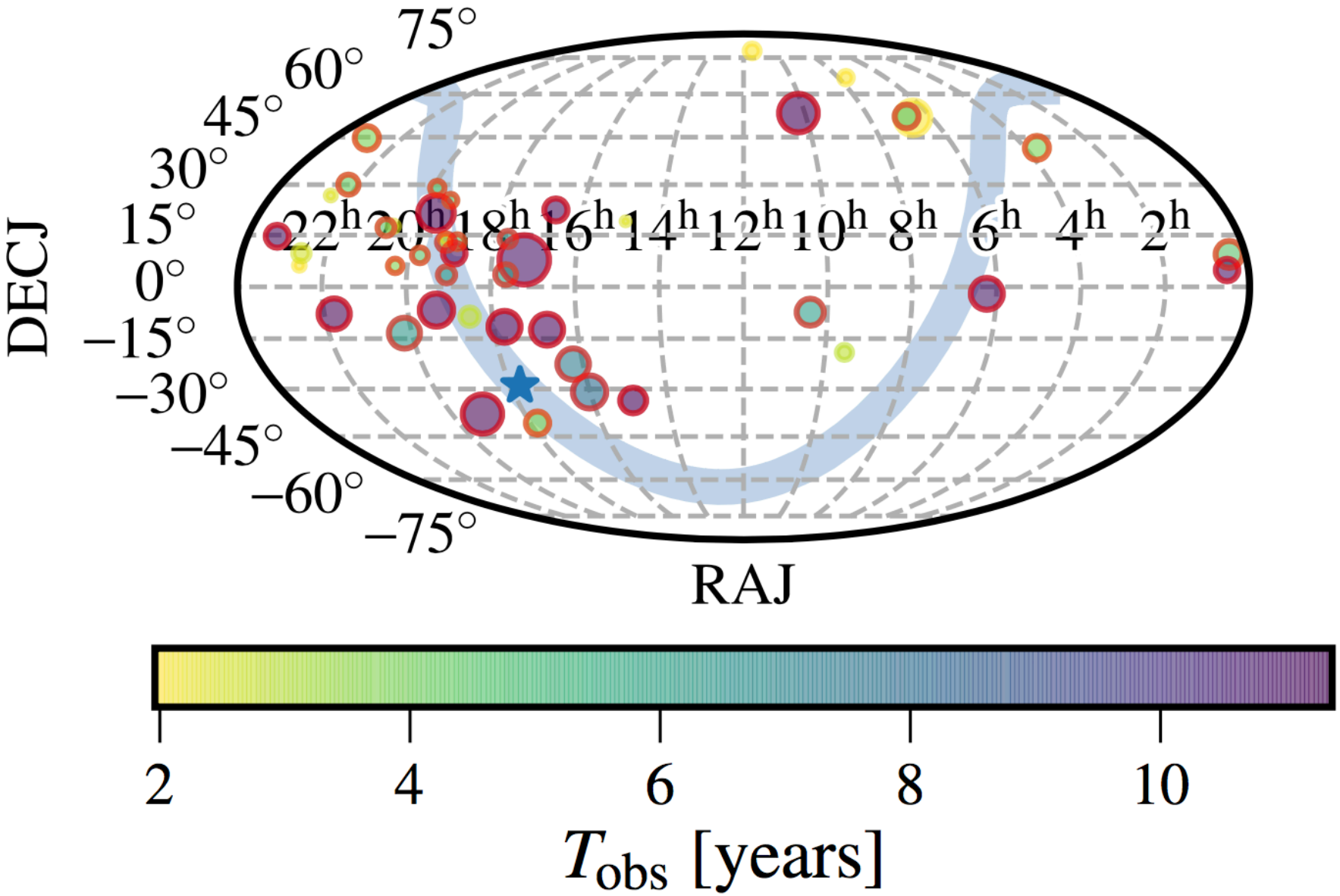

Image: sky map of NANOGrav pulsars in the 11-yr data set

Signal

$$h_c(f) = A_{\rm GWB}\left(\frac{f}{f_{\rm yr}}\right)^{\alpha} \qquad \alpha = -2/3 \text{ for a population of inspiraling SMBHBs}$$

Pulsar residual

$$\langle r_a^*(t_j) r_b(t_k)\rangle = S_{ab}(f) = \Gamma_{ab}\frac{{A_{\rm GWB}}^2}{12\pi^2}\left(\frac{f}{f_{\rm yr}}\right)^{-\gamma} f_{\rm yr}^{-3} \qquad \gamma = 3 - 2\alpha$$

- Monopolar ORF Γ_{ab}=1 (*due to clock error*)
- Dipolar ORF Γ_{ab}= cos ζ (*due to error in solar system ephemeris*)
- Quadupolar ORF Γ_{ab} = HD curve (*genuine GWB signal*)

Noise

white noises (instrumental) + pulsar intrinsic red noise
(including pulsar spin noise, pulsar profile changes, dispersion measure variations,…)

$$N_{aa}(f) = {A_{\rm red}}^2 (f / f_{\rm yr})^{-\gamma} {f_{\rm yr}}^{-3}$$

common-spectrum process across MSPs $S_{aa}(f)$

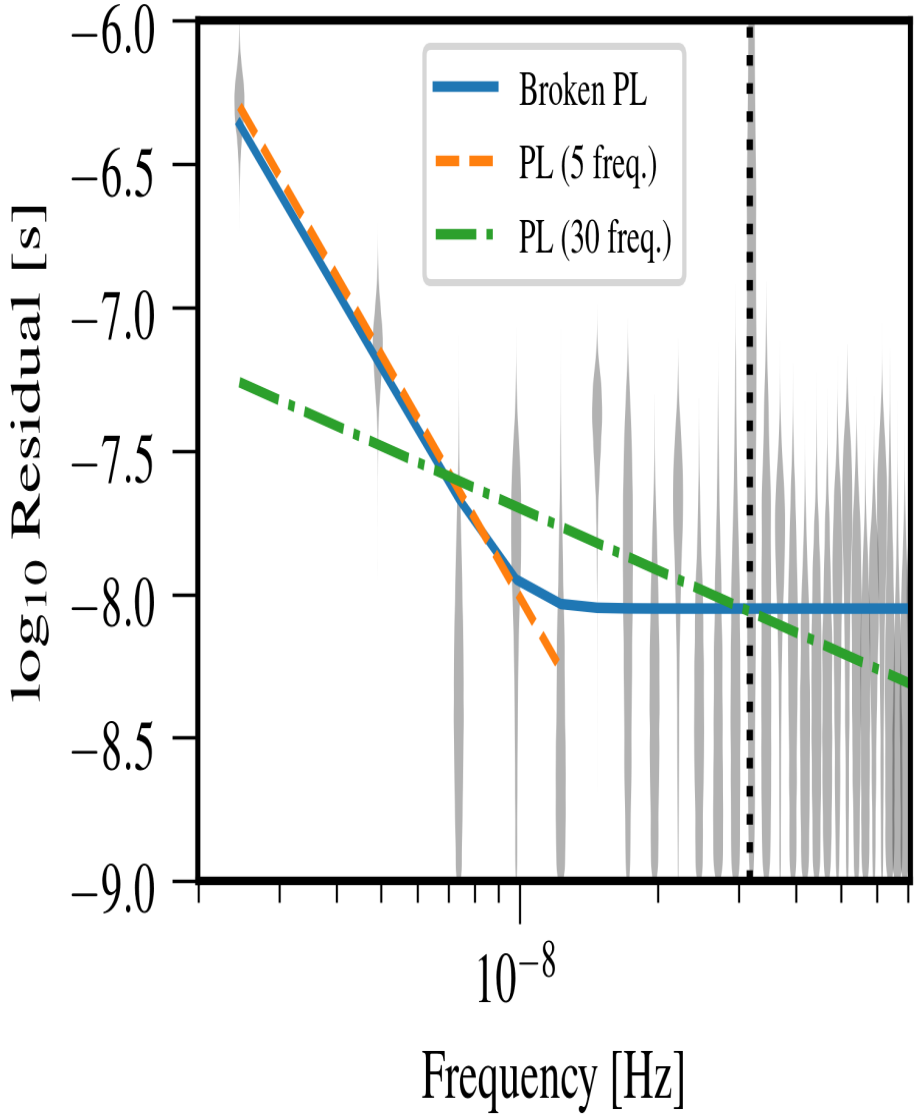

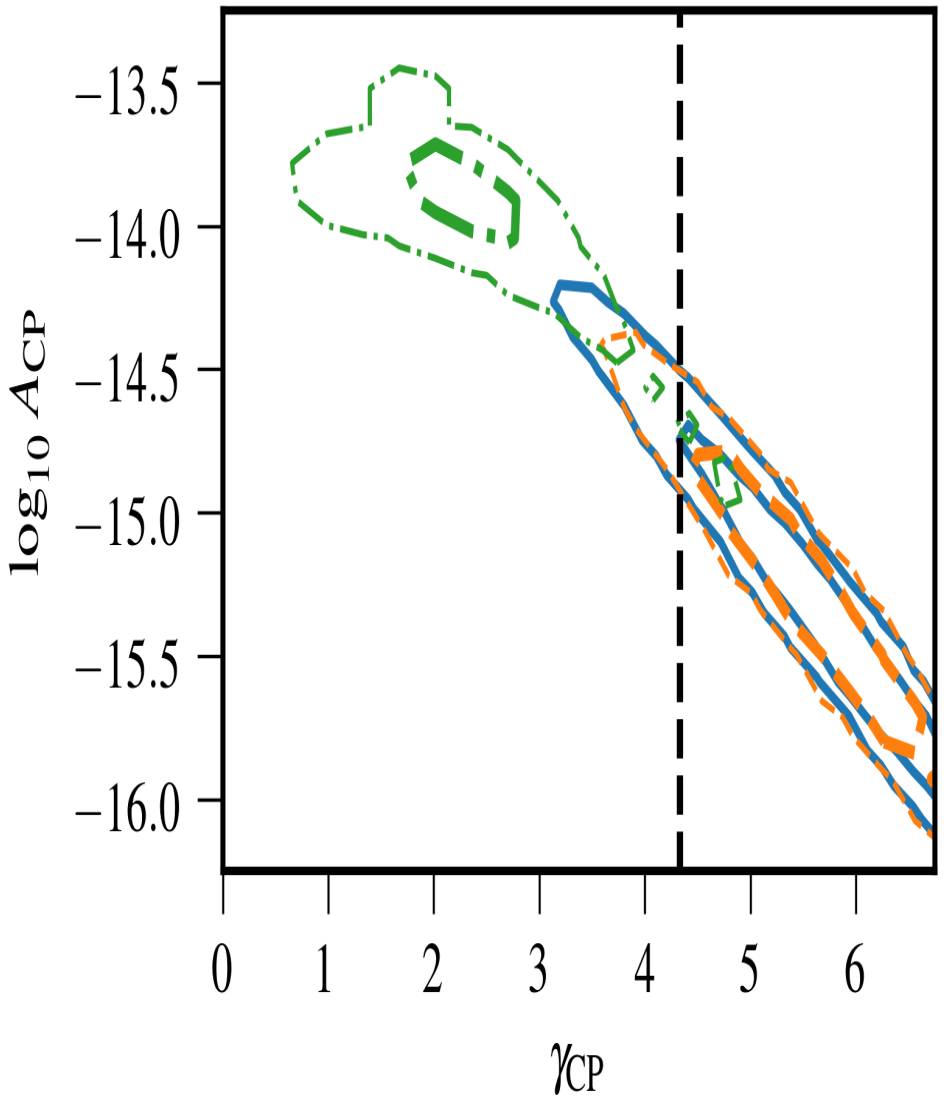

Spatial correlation $S_{ab}(f)$

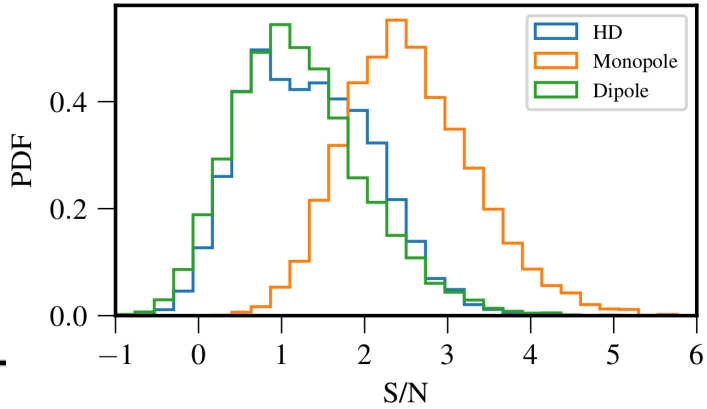

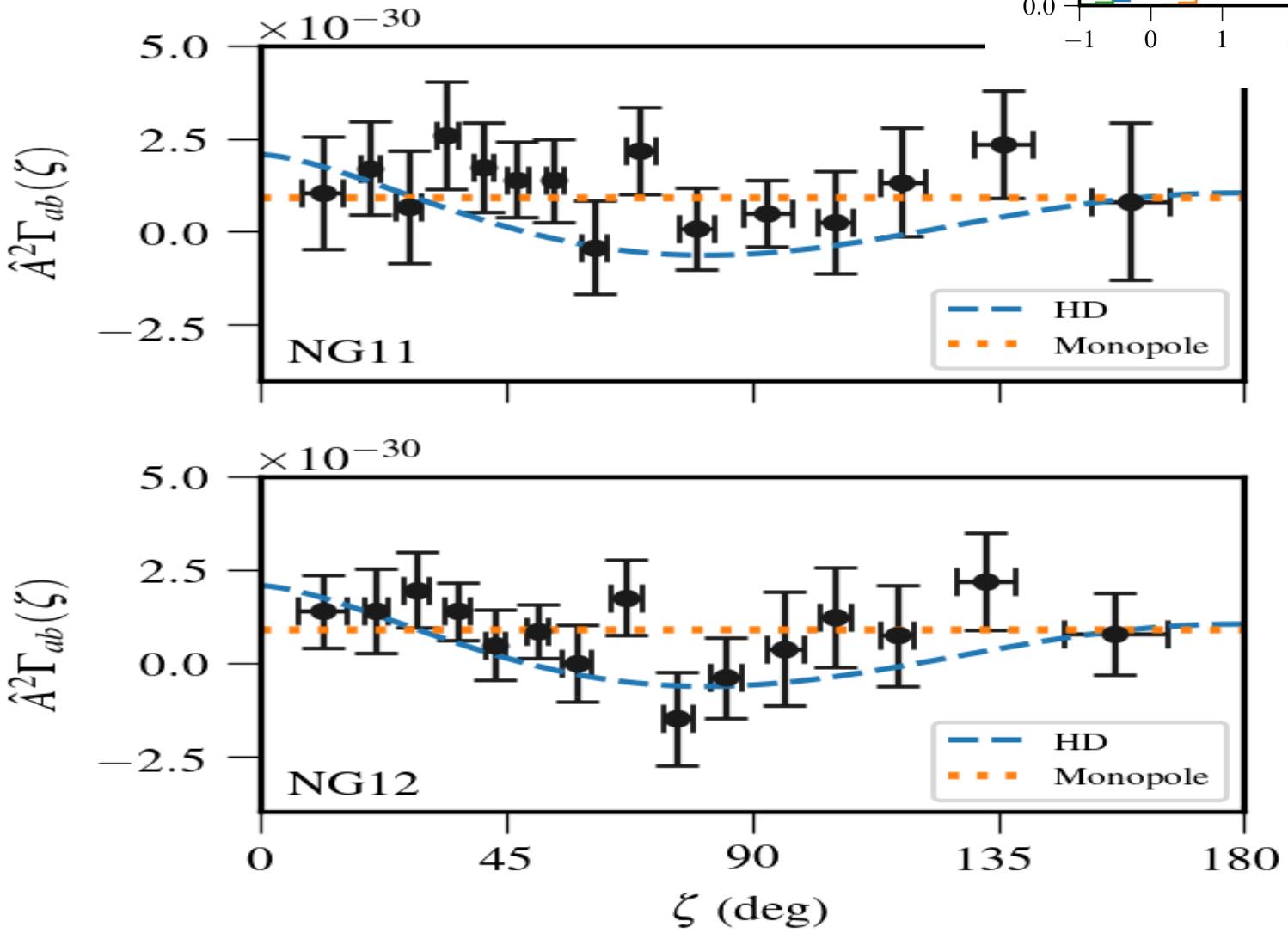

NANOGrav projection

arXiv:2009.04496

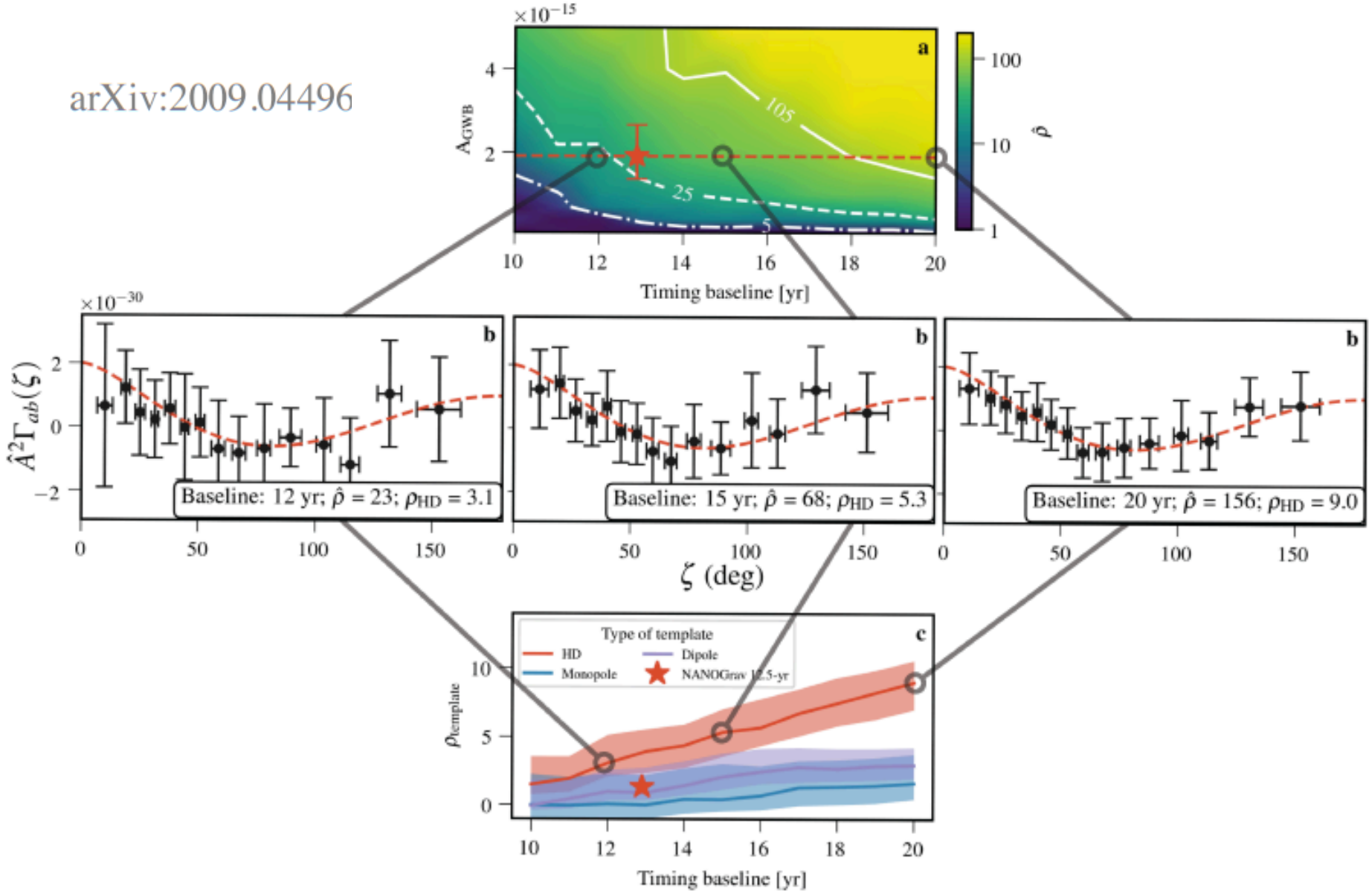

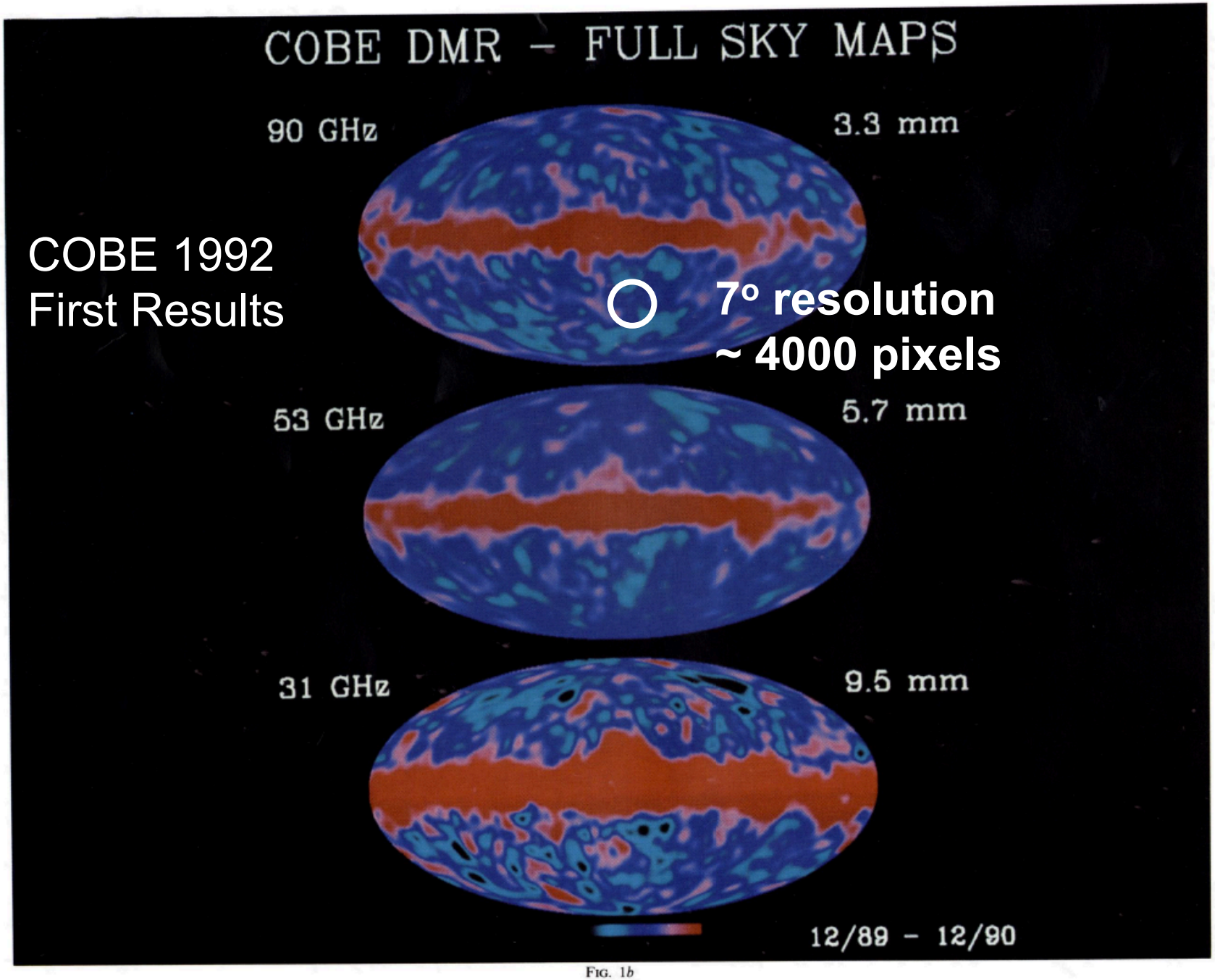

COBE 1992
First Results

7° resolution
~ 4000 pixels

FIG. 1*b*

SMOOT et al. (see 396, L2)

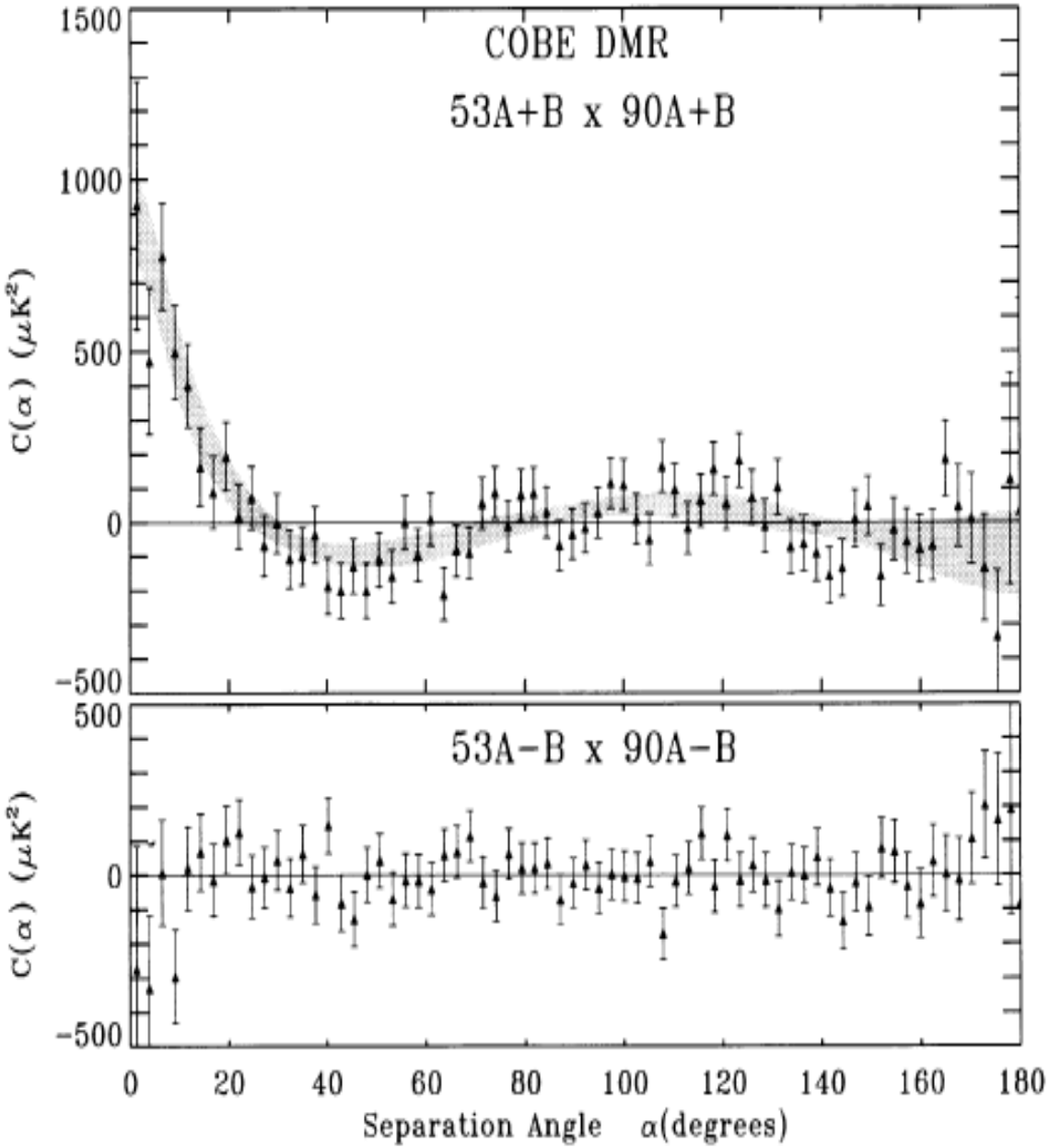

FIG. 3.—Cross-correlation of 53 GHz with 90 GHz for $|b| > 20°$ plus the correlation function for a scale-invariant spectrum with an expected quadrupole amplitude of 15.4 μK: the gray band indicates 68% C.L. cosmic variations. *Top* is for the sum maps, and *bottom* is for the difference maps. The cross and autocorrelations for the various combination of maps all have consistent values.

Future SKA will observe thousands of millisecond pulsars

Power spectrum of the correlation (l-space)

$$\langle r(t_1)r(t_2)\rangle = \int_0^{t_1} dt' \int_0^{t_2} dt'' \langle z(t')z(t'')\rangle$$
$$= \int_0^{t_1} dt' \int_0^{t_2} dt'' e^{-ik_*(t'-t'')} \langle z(\mathbf{e_1})z(\mathbf{e_2})\rangle$$

$$\langle z(\mathbf{e_1})z(\mathbf{e_2})\rangle = \sum_l \frac{2l+1}{4\pi} C_l P_l(\mathbf{e}_1 \cdot \mathbf{e}_2)$$

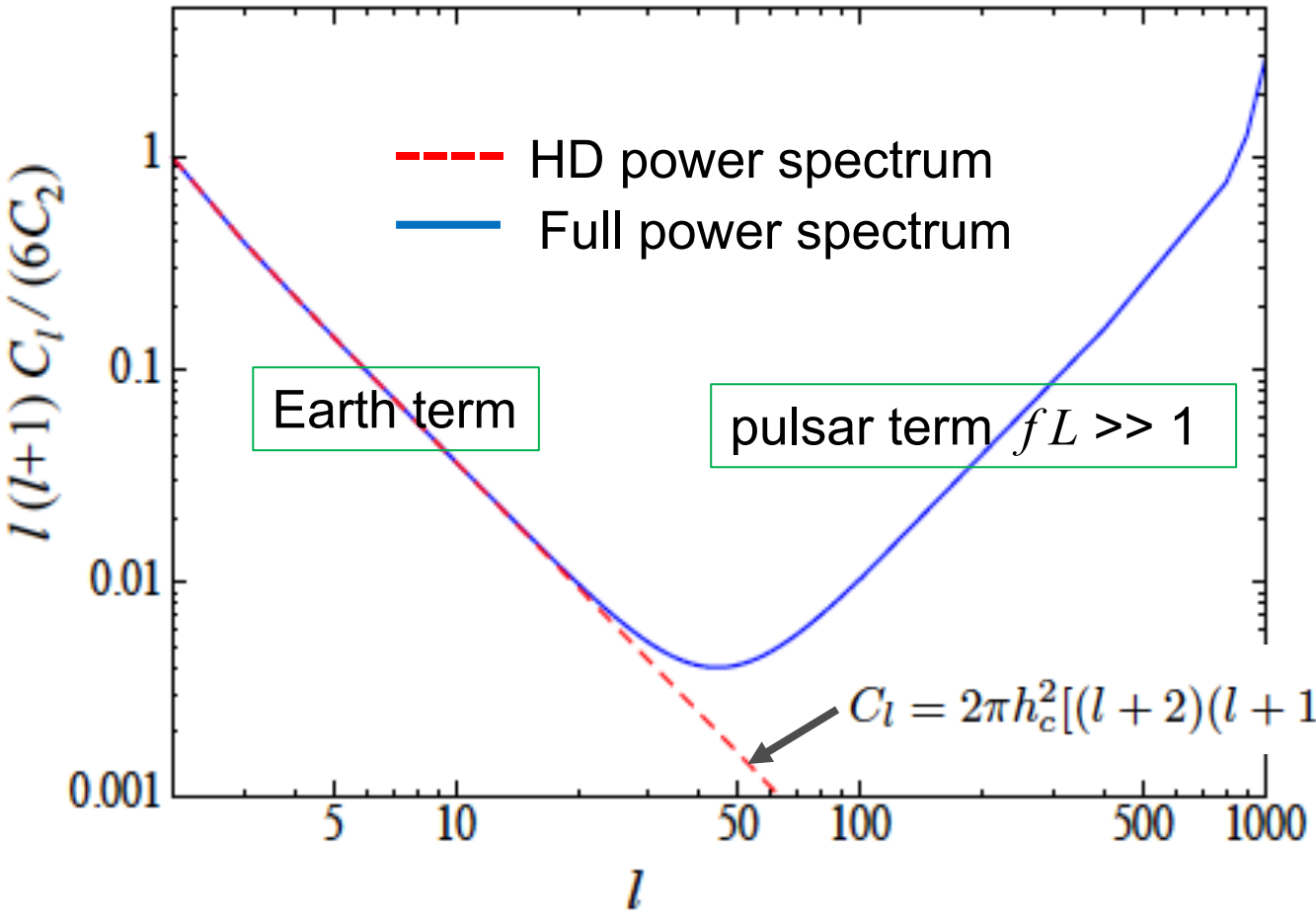

To map this small-scale power needs tens of thousands of MSPs; however, we can search for a signal of close-by pulsar pair in globular clusters

Gaia space optical telescope (2013-2022) for astrometry: measuring the positions, distances and motions of a billion stars with micro arcsecond precision.

The angular deflection of a star in direction **n** due to GWs h_{ij}

$$\delta n^{\hat{i}}(\tau_0, \mathbf{n}) = \frac{n^i + p^i}{2(1 + \mathbf{p}\cdot\mathbf{n})} h_{jk}(0) n_j n_k - \frac{1}{2} h_{ij}(0) n_j$$

for plane waves in the direction **p**. Book+Flanagan 11

Future missions:
NEAT, Theia,..

Gaia map of the sky by star density

Conclusion

- GWB is a main goal in GW experiments
- GWB monopole and Doppler dipole
- GWB anisotropy and polarization
- Correlate with other cosmological data such as LSS, CMB
- GWB is a deep probe into the very early Universe
- NANOGrav and PPTA saw the GW monopole? If so, then the game may have started…

CMB Milestones

1965 **AT&T Bell** Penzias and Wilson

1978
Arno Penzias
Robert Wilson

1992 **NASA** COBE

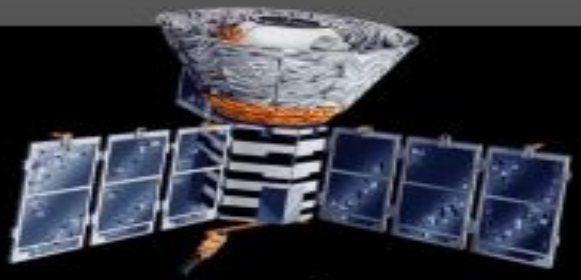

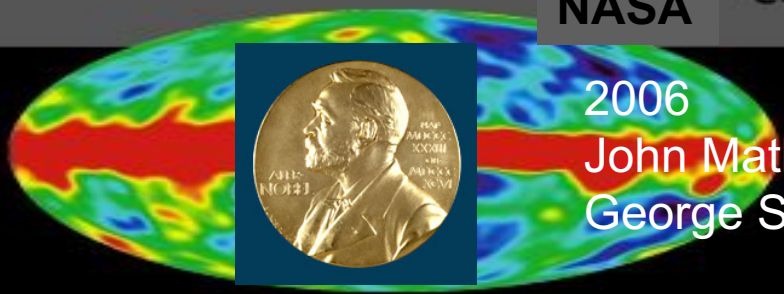

2006
John Mather
George Smoot

2003 **NASA** WMAP

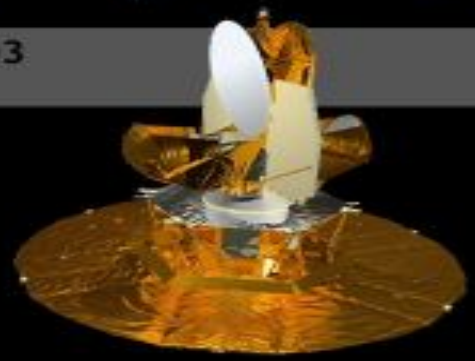

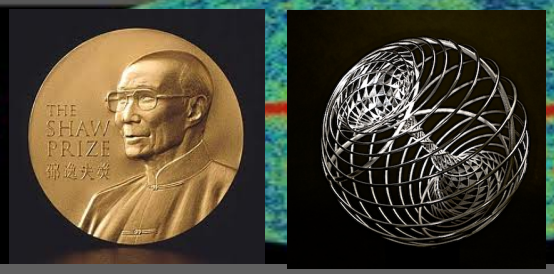

2010, 2018
Charles Bennett
Lyman Page
David Spergel

2013 **ESA** **Planck**

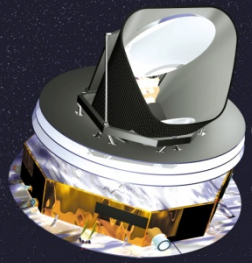

Plus many ground-based experiments

2004, 2019
James Peebles
Theoretical Cosmologist